Journal of
Medicinal Chemistry

Article

Identifying novel anti-osteoporosis leads with a chemotype-assembly approach

Chao Zhao, Dane Huang, Ruyue Li, Yida Xu, shimin su, Qiong Gu, and Jun Xu

J. Med. Chem., **Just Accepted Manuscript** • DOI: 10.1021/acs.jmedchem.9b00517 • Publication Date (Web): 24 May 2019

Just Accepted

is published by the American Chemical Society. 1155 Sixteenth Street N.W., Washington, DC 20036

Identifying novel anti-osteoporosis leads with a chemotype-assembly approach

Chao Zhao[†], Dane Huang[†,‡], Ruyue Li[‡], Yida Xu[†], Shimin Su[†], Qiong Gu*[,†], Jun Xu*[,†,§]

[†]Research Center for Drug Discovery, School of Pharmaceutical Sciences, Sun Yat-Sen University, Guangzhou 510006, China

[‡]Guangdong Province Engineering Technology Research Institute of T.C.M., Guangdong Provincial Key Laboratory of Research and Development in Traditional Chinese Medicine, Guangzhou 510095, China

[§]School of Biotechnology and Health Sciences, Wuyi University, 99 Yingbin Road, Jiangmen 529020, China

ABSTRACT

In this paper, we applied a chemotype-assembly approach for ligand-based drug discovery (LBDD) to discover novel anti-osteoporosis leads. With this new approach, we identified 12 chemotypes and derived 18 major chemotype assembly rules from 245 known anti-osteoporosis compounds. Then, we selected 19 compounds from an in-house compound library using chemotype-assembly approach for anti-osteoporosis assays, which resulted in 13 hits. Based on structural features in these 13 compounds, we synthesized 50 possible anti-osteoporosis compounds from the anti-osteoporosis chemotypes by means of click chemistry techniques and discovered a compound (**10a**, IC_{50} = 2 nM) with nanomolar activity. Compound **10a** was then proved to be a anti-

osteoporosis lead since it can prevent bone loss *in vivo*.

INTRODUCTION

Ligand-based drug discovery (LBDD) is an interesting rational drug design method to accelerate the earlier stages of drug discovery.[1] LBDD usually begins with a collection of known molecules that have the same target or treat same diseases. This collection is then used to perform quantitative structure-activity relationship (QSAR) studies, substructure retrieval or similarity searches against commercial or in-house databases.[2-3] A key limitation of LBDD is that newly identified molecules are often close analogues of known ligands and novelty therefore is limited.

Recently, we reported identification of the privileged fragments (substructures of known compounds) and the assembly rules for liver X receptor-β (LXRβ) from known LXRβ agonists.[4] These fragments and rules are then successfully applied to discover new agonists. This approach encourages us using substructures for LBDD and overcomes the limitations of LBDD. However, a remaining question is whether this approach can be applied to wider range of diseases. This is an important problem since many diseases lack of validated molecular targets.[5] We hypothesize that the active agents related to a disease are constructed from different chemotypes according to some assembly rules. The chemotype is defined as "a chemical structure motif or primary substructure that is common to a group of compounds".[6]

Osteoporosis affects more than 25% of women and more than 10% of men in their lifetimes and is a disease that is characterized by loss of bone mass, leading to increased

risk of fractures. It was selected to test our hypothesis.[7-9] Anti-osteoporosis drugs including bisphosphonates,[10] cathepsin K inhibitors[11] and parathyroid hormone mimetics[12] are available but challenges in osteoporosis therapy still remain, because no drugs have been found that reduce the risk of fractures significantly.[13]

Here we applied a previously described *de novo* substructure generation algorithm (DSGA)[4] to extract privileged fragments from a library of known anti-osteoporosis compounds. DSGA allows us to discover frequent substructures or fragments from a chemical structure library. The fragments that remained after 'rule of 3'[14] filtering were clustered according to our previously described scaffold-based classification approach (SCA).[15] SCA can provide the scaffold and complexity of a structure. The complexity presents the heavy atom number of substituents on this scaffold. These two parameters are applied to cluster the fragments. One cluster was identified as a chemotype[6] and then chemotype assembly rules were generated by analysis of the linkages between two neighboring chemotypes. From the chemotypes and their assembly rules, a series of substructures, which present by Markush queries, were constructed and used to screen our in-house library. A number of candidate lead compounds were identified according to the bioassay results. Further optimization with click reactions and chemotype assembly rules gave a putative anti-osteoporosis lead compound. The flowchart for this process is shown in Figure 1.

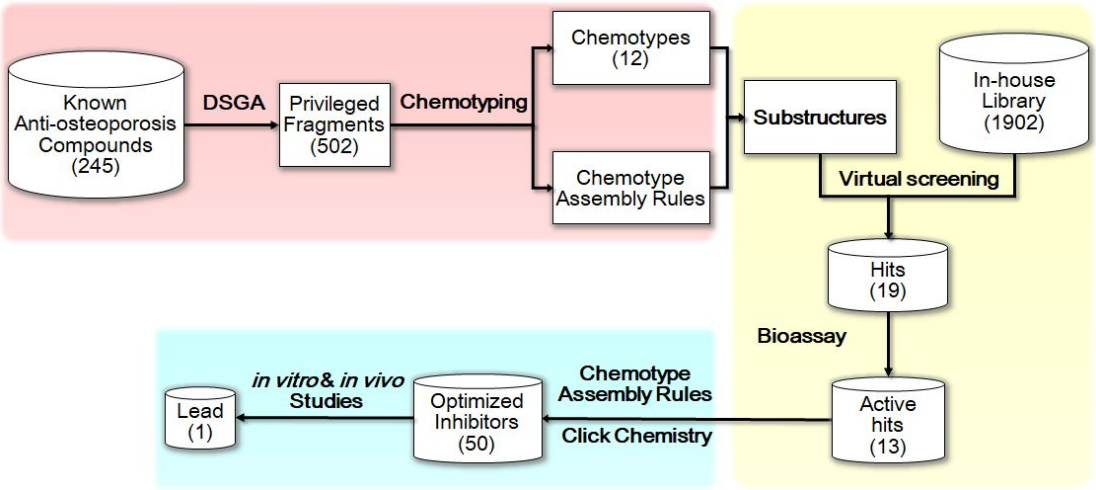

Figure 1. The flowchart of candidate anti-osteoporosis lead discovery through assembly of chemotypes. The process begins with a *de novo* substructure generation algorithm (DSGA) which, after inspection of 245 known anti-osteoporosis compounds identifies 502 chemical fragments. Chemotype analysis permits clustering of the fragments into 12 chemotypes by SCA. By analyzing the linker between two neighboring chemotypes in a known anti-osteoporosis compound, chemotype assembly rules can be defined. Both the chemotypes and rules are used to construct a series of substructure. By searching our in-house library with substructure retrieval, 19 compounds were selected for bioassay. Lead candidates were further optimized by click chemistry and the anti-osteoporosis leads were validated with *in vitro* and *in vivo* experiments.

RESULTS

Chemotypes Derived from Known Anti-osteoporosis Agents. A total of 245 known anti-osteoporosis agents were collected from published sources. These compounds were divided into 28 classes based on their associated targets: 162 compounds have specific protein targets, 19 compounds are involved in signal transduction pathways, 60 compounds are cell-based regulators, and 4 compounds have been tested on animal models but lack target information (Tables S1, S2 in Supplementary Information - SI).

Employing DSGA on this library resulted in 502 privileged fragments (Table S3). According to the "rule of three", fragments were eliminated if: (1) they are acyclic, (2) their molecular weight is >300 and the number of hydrogen bond donors >3 and the

number of hydrogen bond acceptors >3 and cLogP >3,[14, 16] and (3) the smallest set of smallest rings >1.[17] This resulted in 54 fragments, which were classified by SCA into 12 chemotypes (Table 1).

Table 1. Anti-osteoporosis chemotypes, their frequency and appearance in known anti-osteoporosis agents

Chemotype ID[a]	Topology	Frequency	EF[b]	Example molecules	Targets	Ref.
A: C6AR1	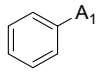	228	1	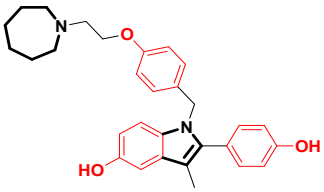 Bazedoxifene	SERM[d]	18
B: C6AR		191	1	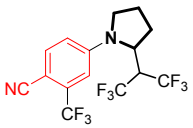 Ligandrol	SARM[e]	19
C: C6AR2	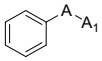	105	1	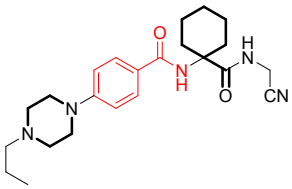 Balicatib	cathepsin K inhibitor	20
D: C5AR		67	1	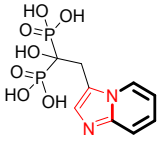 Minodronic acid	BPs[f]	21
E: C6HR		54	1	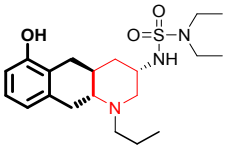 Quinagolide	D2R Agonist[g]	22

F: C6HAR		47	1	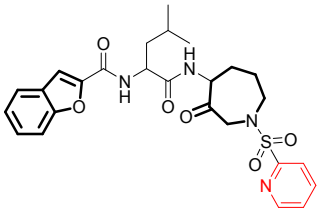 Relacatib	cathepsin K inhibitor	23
G: C6R		54	1	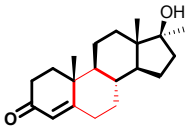 Methyltestosterone	SARM	24
H: C5R		45	1	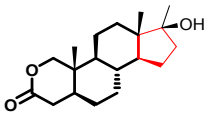 Oxandrolone	SARM	25
I: C6AR3	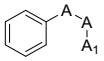	40	1	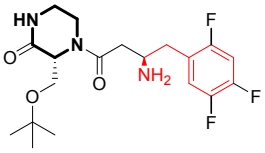 Evogliptin	DPP-IV Inhibitor[h]	26
J: C6RE		34	1	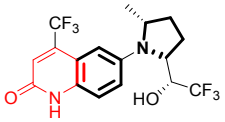 LGD2941	SARM	27
K: C6R1		28	1	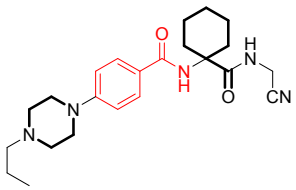 Balicatib	cathepsin K inhibitor	20
L: C7R		10	1	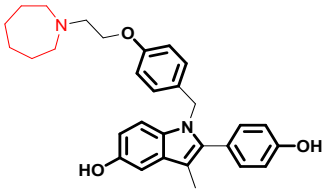 Bazedoxifene	SERM	18

[a]The general formula of chemotype ID is Cm(H)(A)R(n), where C = chemotype, m = number of ring members, H = hetero (not essential), A = aromatic (not essential), R = ring and n = length of side chain (not essential). [b]EF = enrichment factor. [c]The meaning of letters in topology structures: A = C, O, N, S, CO, SO_2; A_1 = non-terminal groups, such as O, N, S, CO, SO_2; T = terminal substituents, such as H, Cl, F, Br, CF_3, CN, NO_2; A-A_1 or A-A can be C=C, C≡C; Q = non-carbon heavy atom, such as O, N, S. [d]SERM = selective estrogen-receptor modulator. [e]SARM = selective androgen-receptor modulator. [f]BPs = bisphosphonates.

[g]D2R agonist = dopamine receptor D_2 agonist. [h]DPP-IV inhibitor = dipeptidyl peptidase-4 inhibitor.

As shown in Table 1, a chemotype is a core to a fragment family, in which ring can be a part, but a chemotype is not equivalent to a ring. One compound usually constructed by two or more chemotypes. For example, bazedoxifene, a selective estrogen receptor modulator, consists of 5 chemotypes (3 x C6AR1, 1 x C7R, and 1 x C5AR (Table 1 row 1); The cathepsin K inhibitor, balicatib consists of 3 chemotypes (1 x C6HR, 1 x C6AR2, and 1 x C6R1 (Table 1 row 3) and methyltestosterone consists of 4 chemotypes (1 x C6RE, 2 x C6R, and 1 x C5R (Table 1 row 7). The enrichment factor (EF) of the chemotypes were calculated by following formulas[28]:

$$EF = (Ha \times D) \div (Ht \times A)$$

Where, Ht = total number of compounds with selected chemotype, Ha = the total number of active molecules in the Ht, D = total number of molecules in library, and A = the total number of actives in the database.

Chemotype Assembly Rules Derived from Known Anti-osteoporosis Agents. The assembly rules define two chemotypes and the linker between them. To explore chemotype assembly rules systematically, we use the substructures which present chemotypes as queries against the known anti-osteoporosis molecules. For the two chemotype combinations, there are $C_{12}^2 + 12 = 78$ queries, including homo- and hetero-combinations, and these queries were used to retrieve compounds from the anti-osteoporosis library. The structural moiety connecting two neighboring chemotypes is identified as the linker and an example is described in Figure 2. In this way, a total of five different linkers, shown in Figure 2 were identified. These are coupling (L1), two

chemotypes directly connected; alkane chain (L2), two chemotypes connected by an alkyl chain with 1-3 carbons; carbonyl containing chain (L3), two chemotypes connected by an alkyl chain with 1-3 carbons and containing a carbonyl group, such as ketone, amide or ester; ring fusion (L4), two chemotypes form one fused ring; and ring merging (L5), two 6 member ring overlapped to give a multisubstituted ring. Theoretically, there are 78×5 or 390 assembly rules. Analysis of the anti-osteoporosis library resulted in 131 assembly rules, and their frequencies were also calculated (Figure S1). The assembly rules with L1 ~ L3 usually construct the scaffold,[29-30] L4 provides fused ring and rules involving L5 provide multisubstituted rings. Therefore, L1~L3 are preferred for discovering new scaffold leads.

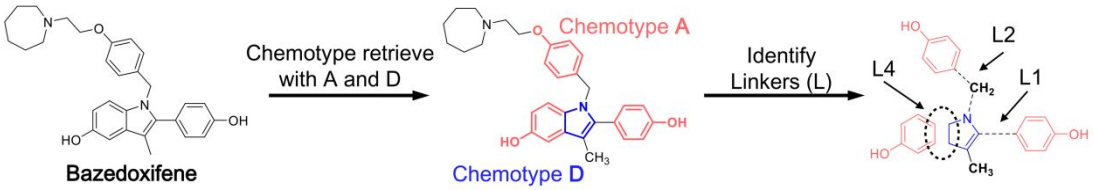

Linker 1 (L1)	Linker2 (L2)	Linker 3 (L3)	Linker 4 (L4)	Linker 5 (L5)
Coupling	A=C, N, O, S n = 0 ~ 3	X = O, N, S Y = O, N, S, C m, n = 0 - 1	Ring Fusing	Ring Merging

Figure 2. Linker identification process and assembly rules. Analysis of assembly rules with bazedoxifene. (1) Results of chemotype substructure retrieval, red represents chemotype A; blue represents chemotype D. (2) Identification of the linkers, L1, L2 and L4.

Performance Validation of the Chemotype Assembly Rules. A library of chemicals associated with chemotype A consisting of 32 anti-osteoporosis compounds was curated from published papers. The decoy library (8,558 compounds) was constructed with the following procedure: 8,558 compounds (known drugs or agents under clinical trials) were derived from DrugBank database. Anti-osteoporosis

compounds were excluded. The two libraries were combined to form an external testing data set of 8,590 compounds for validation of the performance of the chemotype assembly rules in the anti-osteoporosis lead discovery process. To test whether assembly rules are more efficient than other approaches, single chemotype A (method a), chemotype A with one other chemotype (method b) and substructures constructed according to assembly rules were all used for screening against this test set. As shown in Figure 3A, there are 3,630 molecules containing chemotype A in the test set (blue in Figure 3A). Among these, 32 compounds are anti-osteoporosis agents (green). When method b was applied, the number of retrieved molecules was reduced to 3,618 (yellow) including all 32 osteoporosis agents. When the assembly rules of chemotype A were applied (red), the number of retrieved molecules was significantly reduced to 610, still including the 32 known osteoporosis agents. The hit rates of three methods are 0.88%, 0.88% and 5.25% respectively (Figure 3A). Thus, when assembly rules were applied, the hit rate was increased more than 5 times. This validation was also applied to chemotype D and chemotype H. A total of 28 anti-osteoporosis compounds associated with chemotype D and decoys were used in the validation test (Figure 3B). The hit rates of method a, method b and chemotype D with assembly rules are 1.43%, 1.57% and 5.02% respectively. These results show that assembly rules of chemotype D increase the hit rate by a factor of >3. A total of 8 chemotype H associated anti-osteoporosis compounds and decoys were used in the validation test (Figure 3C). The hit rate of chemotype H with assembly rules is 4.82%, about 10 times that of other 2 methods. These data indicate that assembly rules can increase the efficiency in hit discovery. The EF of our approach is also increased significantly compare to other two methods. Accordingly, the chemotype-assembled substructures based on associated rules were applied to the discovery of anti-osteoporosis leads.

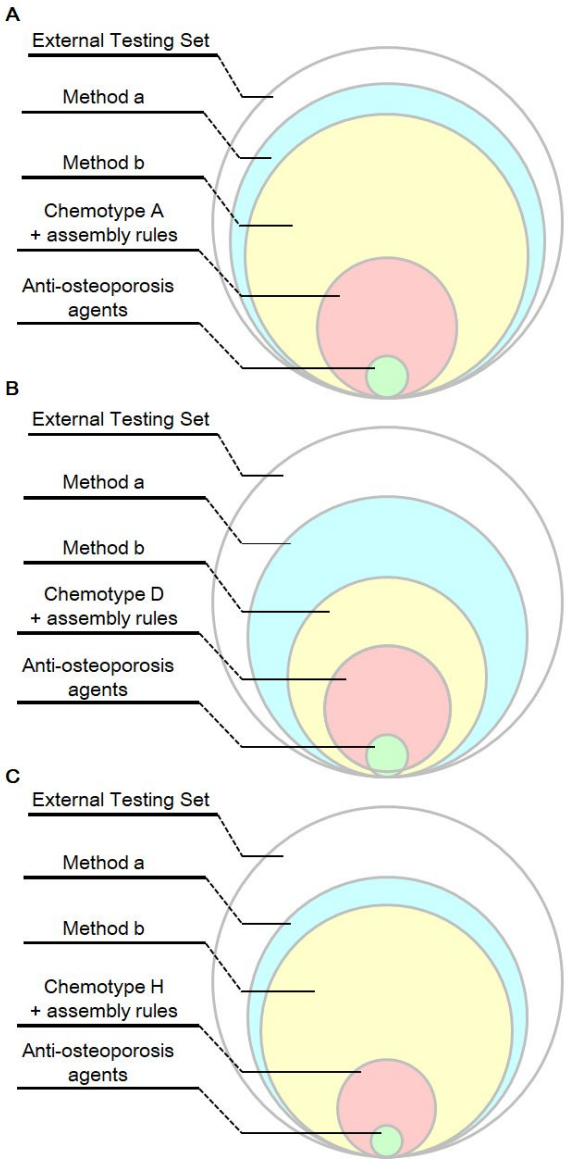

Parameters	Screening method		
	Method a	Method b	Chemotype A + assembly rules
D	8590	8590	8590
A	32	32	32
Ha	32	32	32
Ht	3630	3618	610
Hit rate	0.88%	0.88%	5.25%
EF	2.37	2.37	14.08

Parameters	Screening method		
	Method a	Method b	Chemotype D + assembly rules
D	8586	8586	8586
A	28	28	28
Ha	28	28	27
Ht	1960	1788	538
Hit rate	1.43%	1.57%	5.02%
EF	4.38	4.80	15.39

Parameters	Screening method		
	Method a	Method b	Chemotype H + assembly rules
D	8566	8566	8566
A	8	8	8
Ha	8	8	8
Ht	1774	1663	166
Hit rate	0.45%	0.48%	4.82%
EF	4.83	5.15	51.60

Figure 3. Results of ligand-based virtual screening against an external test set. (A) Screening with chemotype A and its assembly rules. (B) Screening with chemotype D and its assembly rules. (C) Screening with chemotype H and its assembly rules. The screening with assembly rules increased the hit rate by ~3 compared to other methods. The meaning of abbreviations in the Tables: D = number of molecules in the external testing set; A = number of active compounds in the external testing set. Ha = number of active molecules in the hit list; Ht = number of hit molecules from the database. Hit rate = [(Ha/A) × 100]. EF = enrichment factor.

Identification of Anti-osteoporosis Lead Candidates through Screening against an In-house Compound Library using Chemotype D Assembly Rules. Chemotype

D and its assembly rules with L1~L3 was selected for further study for two reasons because chemotype D has a high frequency of occurrence, more than one fourth of anti-osteoporosis compounds contain chemotype D. Moreover, many clinical and commercial anti-osteoporosis drugs including strontium ranelate, raloxifene, bazedoxifene and relacatib are constructed by chemotype D. A second reason is that chemotype D represents 5-membered aromatic rings, such as triazole, which can be prepared by one step click chemistry. As shown in Figure 4A, chemotype D has 18 different assembly rules with chemotypes A, B, C, D, E, F, G, H, I, J and L and L1 ~ L3. For further study, we selected the most important assembly rules of chemotype D with each of the chemotypes, including 'D+L1+A', 'D+L1+B', 'D+L1+C', 'D+L3+D', 'D+L3+E', 'D+L1+F', 'D+L3+F', 'D+L1+G', 'D+L2+G', 'D+L2+H', 'D+L1+I', 'D+L2+I' (Figure 4B). These assembly rules were then applied to construct a set of substructures for drug discovery (Table 3).

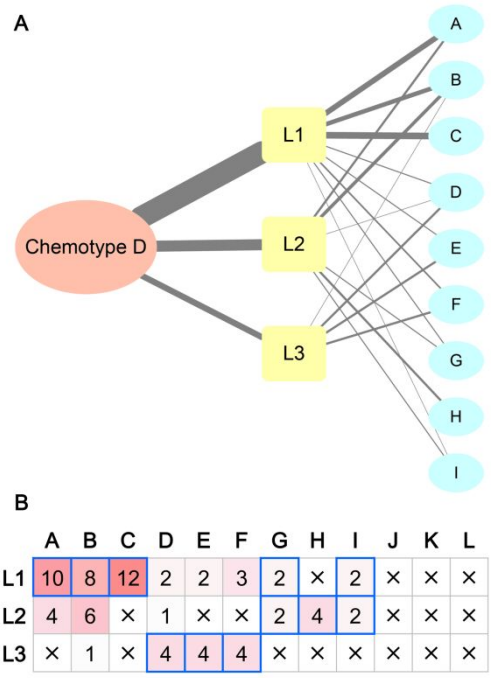

Figure 4. (A) The assembly rules of chemotype D. The thickness of line represents the degree of use of assembly rules, the thicker of line, the more frequent use of assembly rules. (B) Assembly rules between chemotype D and other chemotypes with L1~L3. The numbers in the box represent the instance of assembly rules. 'X' represents that there is no connection between two chemotypes.

Table 3. Substructures constructed by chemotype D assembly rules

ID	Substructures	Assembly rules
Q1	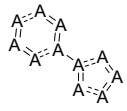	D+L1+A D+L1+B D+L1+C D+L1+F
Q2	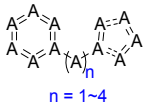	D+L1+A D+L1+C D+L1+I D+L2+I
Q3	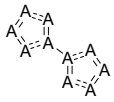	D+L1+D
Q4	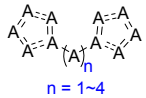	D+L3+D
Q5	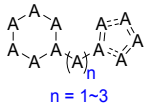	D+L3+E D+L3+F D+L2+G

Q6	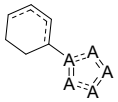	D+L1+G
Q7	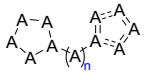 n = 1~4	D+L2+H

Here, our in-house library containing 1,902 compounds were applied to discover anti-osteoporosis hit compounds. The in-house library consists of 321 natural products and 1581 synthetic compounds with 901 different scaffolds, and 41 compounds that have a thiazole amide substructure. The substructures were then used to search for compounds against osteoporosis in this library through substructure retrieve. After removal of duplicates, this gave 128 compounds with 30 different scaffolds. After comparison with known anti-osteoporosis agents, 19 hit compounds with novel scaffolds (Figure S2) remained and were tested against receptor activator of nuclear factor-kappa B ligand (RANKL)-induced bone marrow macrophage cells (BMMs). Of these, 13 compounds were confirmed as anti-osteoporosis active hits with IC_{50} values $\leqslant$10 μM (Table 4). Primary structure-activity relationship (SAR) studies on the hits show that one of the privileged substructures leading to the active compounds is either the thiazole amide (red in Table 4) or the thiophene amide (red). In our in-house library, only 41 compounds have a thiazole amide substructure. Here, 12 of them were tested and 10 showed activity. The **XOS00048** and **XOS00881** which also contain thiazole amide exhibited no inhibition effects. This may be caused by the dioxole and nitrile groups, since dioxole group is more rigid (**XOS00048** vs. **XOS00057**) and nitrile group is a potent electron withdrawing group compare to ethoxyl group on **XOS00057**. These data

suggest that further optimization of the thiazole amide compounds may afford anti-osteoporosis leads.

Table 4. Structure and anti-osteoclastogenesis activity of selected compounds obeying chemotype D assembly rules

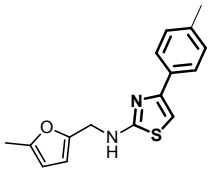 **XOS00702** 1.19 ± 0.26 μM[a]	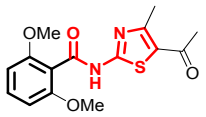 **XOS00055** 2.14 ± 0.33 μM[a]	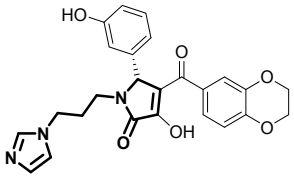 **XOS00011** 2.70 ± 0.18 μM[a]	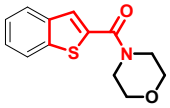 **XOS00700** 3.15 ± 1.01 μM[a]
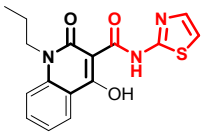 **XOS00046** 3.98 ± 0.85 μM[a]	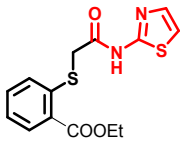 **XOS00049** 3.98 ± 1.44 μM[a]	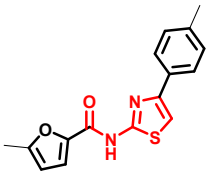 **XOS00056** 4.03 ± 0.87 μM[a]	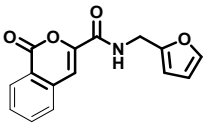 **XOS00033** 4.24 ± 1.71 μM[a]
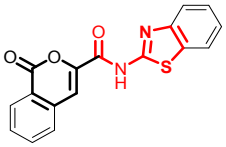 **XOS00036** 5.13 ± 1.06 μM[a]	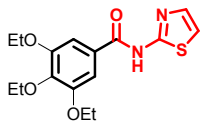 **XOS00057** 6.75 ± 1.15 μM[a]	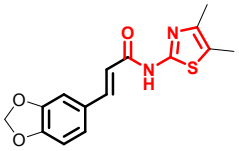 **XOS00063** 8.11 ± 0.99 μM[a]	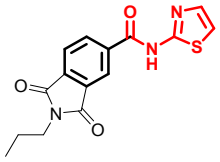 **XOS00067** 10.01 ± 2.13 μM[a]
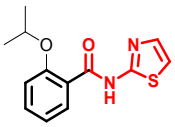 **XOS00064** 12.59 ± 2.15 μM[a]	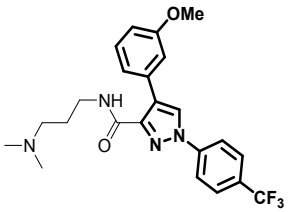 **XOS00281** Inactive[b]	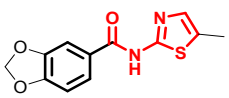 **XOS00048** Inactive[b]	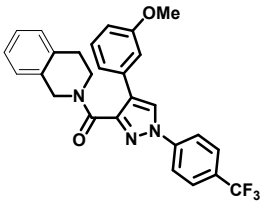 **XOS00189** Inactive[b]
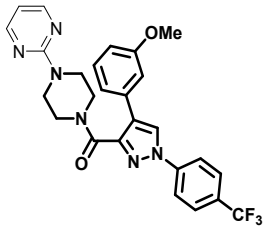 **XOS00280** Inactive[b]	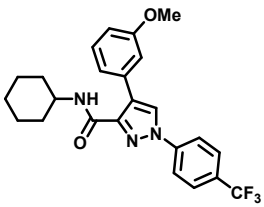 **XOS00285** Inactive[b]	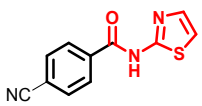 **XOS00881** Inactive[b]	

[a]Activity data are IC_{50} values against RANKL-induced BMM cells. [b]Inactive means that compounds have IC_{50} values >30 μM.

Optimization of Lead Candidates with Assembly Rules and Click Chemistry. According to the assembly rule 'D+L3+D', a thiazole amide is constructed with a triazole ring. A molecule with these three chemotypes can be easily prepared by click chemistry. As shown in Figure 5, there are four kinds of scaffold that can be made in this way, and scaffold IV was chosen based on the availability of starting materials and ease of synthesis. Chemotypes A, B, C, D, and F were applied as the third chemotype assembled with a triazole ring through L1.

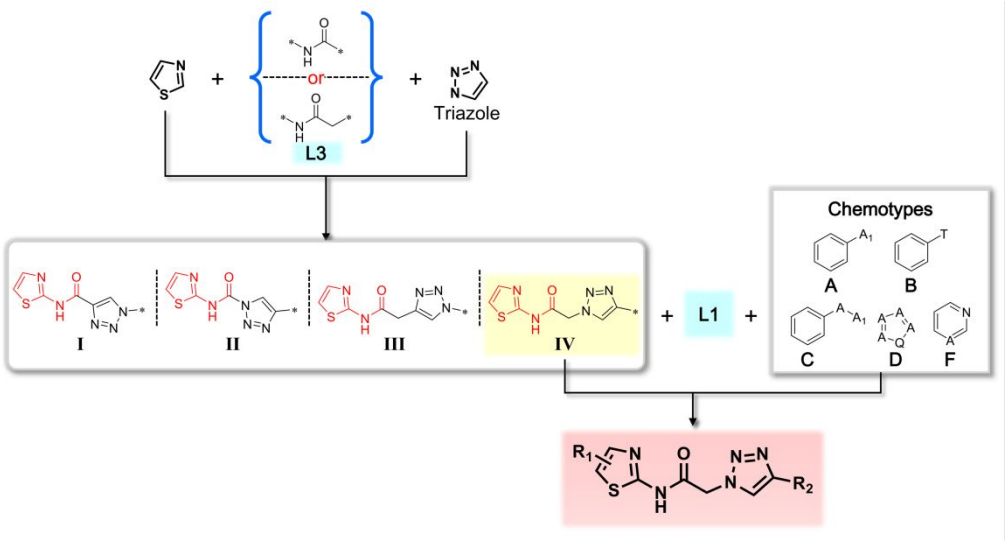

Figure 5. Design of new compounds with thiazole amide (red) according to assembly rules.

In the synthetic strategy shown in Scheme 1, we acquired 5 reagents for R_1, and 13 reagents for R_2 and 50 new compounds were synthesized.

Scheme 1. Synthesis of compounds **6-10**.

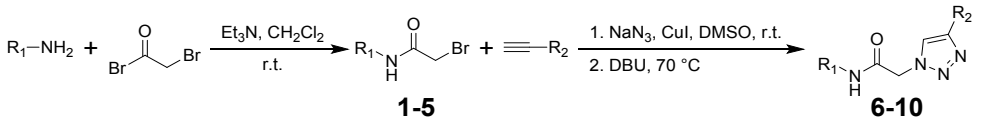

In Table 5, series **6** was assembled with different substituted thiazole or isoxazole amides as R_1 and R_2 as chemotype A. Two different chemotypes A (*p*-methoxyphenyl and *m*-aminophenyl) were introduced, and total of 8 compounds were obtained. Osteoclastogenesis assay of these compounds on BMMs indicated that the isoxazole ring-containing compound **6e** is inactive, but the remaining compounds have IC_{50} values in the range of 0.25~3.89 μM .

Table 5. The structures of compounds **6a-6h** and their activity of anti-osteoclastogenesis

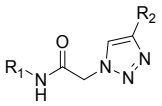
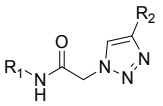

Compd.	R_1	R_2	IC_{50} (μM)[a, b]	Compd.	R_1	R_2	IC_{50} (μM)[a, b]
6a		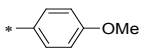	0.51 ± 0.15	**6e**		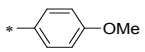	Inactive[c]
6b		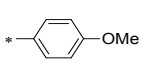	3.89 ±1.44	**6f**		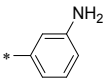	1.27 ± 0.31
6c	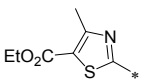	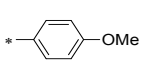	2.33 ± 1.31	**6g**		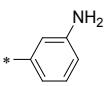	0.25 ± 0.06
6d	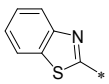	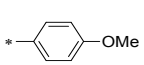	1.33 ± 0.58	**6h**	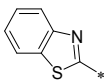	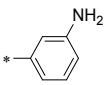	1.11 ± 0.39

[a]Concentration (μM) for 50% inhibition of osteoclast differentiation in RANKL-induced BMMs. The IC_{50} values are the mean ± SEM from at least three experiments. [b]All active compounds were tested at a non-cytotoxic concentration and their CC_{50} values have been provided in the SI (Table S4). [c]Inactive means that compounds have IC_{50} values >30 μ M.

Compounds in series **7** were assembled with substituted thiazole or isoxazole amides and 7 different chemotypes B. A total of 26 compounds were synthesized (Table 6), and 19 of them were active, with IC_{50} values in the range 0.06~9.32 μM. All the chemotypes B except *m*-chlorophenyl exhibited good activity. Thiazole and *o*-chlorophenyl combined to form a potent compound (**7t**) with an IC_{50} value of 0.06 μM. A hydroxyapatite resorption assay indicated that **7t** can discourage osteoclast function significantly (Figure S3). Compounds containing benzothiazole and isoxazole moieties (**7m**, **7n**, **7r**, **7s**, **7w** and **7x**) show little or no activity.

Table 6. The structures of compounds **7a-7z** and their anti-osteoclastogenesis activity

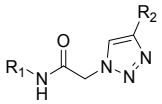

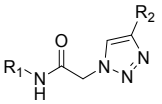

Compd	R_1	R_2	IC_{50} (μM)[a, b]	Compd	R_1	R_2	IC_{50} (μM)[a, b]
7a		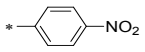	1.04 ± 0.22	**7n**			9.32 ± 1.38
7b		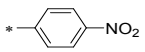	0.19 ± 0.44	**7o**			0.19 ± 0.06
7c	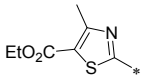	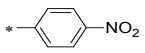	1.84 ± 0.45	**7p**			0.25 ± 0.06
7d	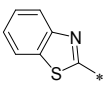	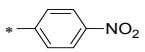	3.28 ± 0.74	**7q**	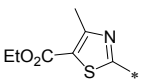		0.66 ± 0.22
7e		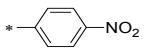	1.22 ± 0.60	**7r**	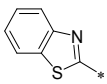		Inactive[c]
7f		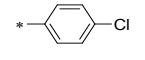	1.10 ± 0.29	**7s**			Inactive[c]
7g		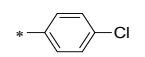	0.52 ± 0.11	**7t**			0.06 ± 0.01

7h	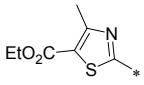	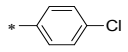	0.18 ± 0.05	**7u**			1.24 ± 0.33
7i	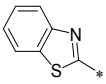	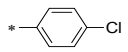	0.13 ± 0.03	**7v**	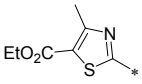		0.13 ± 0.04
7j		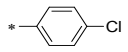	1.91 ± 0.71	**7w**	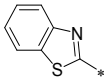		Inactive[c]
7k		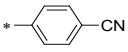	0.27 ± 0.09	**7x**			Inactive[c]
7l	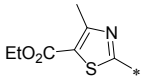	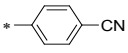	0.31 ± 0.13	**7y**		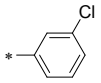	Inactive[c]
7m	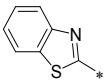	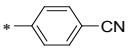	Inactive[c]	**7z**		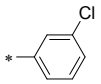	Inactive[c]

[a]Concentration (μM) for 50% inhibition of osteoclast differentiation in RANKL-induced BMMs. The IC_{50} values are the mean ± SEM from at least three experiments. [b]All active compounds were tested at a non-cytotoxic concentration and their CC_{50} values have been given in SI (Table S4). [c]Inactive means that compounds have IC_{50} values >30μM.

Compounds **8a-8f** are constructed with 3 different chemotypes C, including *p*-carbomethoxyphenyl, a *p*-phenylcarboxylic acid and a *p*-ethylnylphenyl group (Table 7). The bioassay results indicated that chemotype C shows no anti-osteoclastogenesis activity.

Table 7. The structures of compounds **8a-8f** and their anti-osteoclastogenesis activity

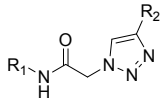

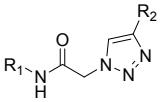

Compd	R_1	R_2	IC_{50} (μM)[a, b]	Compd	R_1	R_2	IC_{50} (μM)[a, b]
8a		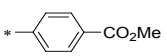	Inactive[c]	**8d**		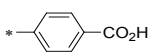	Inactive[c]

8b	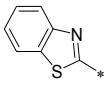	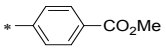	Inactive[c]	**8e**		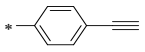	Inactive[c]
8c		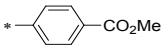	Inactive[c]	**8f**		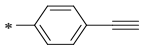	Inactive[c]

[a]Concentration (μM) for 50% inhibition of osteoclast differentiation in RANKL-induced BMMs. The IC_{50} values are the mean ± SEM from at least three experiments. [b]All active compounds were tested at a non-cytotoxic concentration and their CC_{50} values are given in the SI (Table S4). [c]Inactive means that compounds have IC_{50} values >30μM.

Table 8 shows compounds assembled with chemotypes D or F (**9-10**). A total of 5 compounds (**9a-9e**) have chemotype D**,** and 2 of these exhibit potent activity with IC_{50} values of 0.04 μM (**9b**) and 0.02 μM (**9c**) respectively. Compounds **10a-10e**, which were constructed using chemotype F showed the most potent anti-osteoclastogenesis effects compared to other chemotypes. All the compounds showed potent activity with IC_{50} values in the range 0.002-0.43μM. Among all the newly synthetic compounds, compound **10a** exhibited most potent activity with IC_{50} = 0.002 μM. Compound **10a** showed 50-fold increase in potency compare to **10b**. However, the difference of **10a** and **10b** is only a methyl group. This is an example of the activity cliff, which is mainly caused by LogP changes (0.97 for **10a** and 1.7 for **10b**). Also, the methyl group at **10b** may cause a steric clash against the receptor. Thus, the binding affinity of **10b** and its receptor is significantly reduced.

Table 8. The structures of compounds **9-10** and their anti-osteoclastogenesis activity

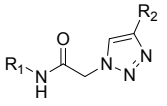

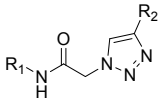

Compd	R_1	R_2	IC_{50} (μM)[a, b]	Compd	R_1	R_2	IC_{50} (μM)[a, b]

9a			Inactive[c]	**10a**			0.002 ± 0.0007
9b			0.04 ± 0.008	**10b**			0.10 ± 0.035
9c	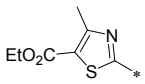		0.02 ± 0.006	**10c**	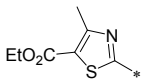		0.12 ± 0.05
9d	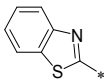		21.35 ± 5.57	**10d**	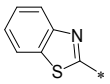		0.05 ± 0.02
9e			Inactive[c]	**10e**			0.43 ± 0.11

[a]Concentration (μM) for 50% inhibition of osteoclast differentiation in RANKL-induced BMMs. The IC_{50} values are the mean ± SEM from at least three experiments. [b]All active compounds were tested at a non-cytotoxic concentration and their CC_{50} values have been given in SI (Table S4). [c]Inactive means that compounds have IC_{50} values >30μM.

In an effort to understand that how chemotypes affect anti-osteoclastogenetic activity, we conducted a chemotype-activity relationship (CAR) analysis. Our current scaffold consists of a thiazole amide and a triazole linker with a group R, which is in a position where new chemotypes could be introduced (Figure 6). Based on the aforementioned assembly rules and the experimental results, chemotypes A, B, D and F have a positive impact on the activities and these effects, by magnitude are in the order F >D >B >A, blue in Figure 6. On the other hand, chemotype C would nullify the desired activities. Conventional SAR studies have also been conducted on these active compounds (yellow). For chemotypes A, B, and F, adding groups at positions 2' and 4' can increase the activity, but adding groups to chemotype B at the 3' position can diminish or eliminate the desired activity. Substituent groups in the thiazole amide ring do not significantly affect the activity, but replacing thiazole by isoxazole significantly reduces or eliminates the activity. By analyzing the results of CAR and SAR, new lead

optimizations are developed and can be used in future studies.

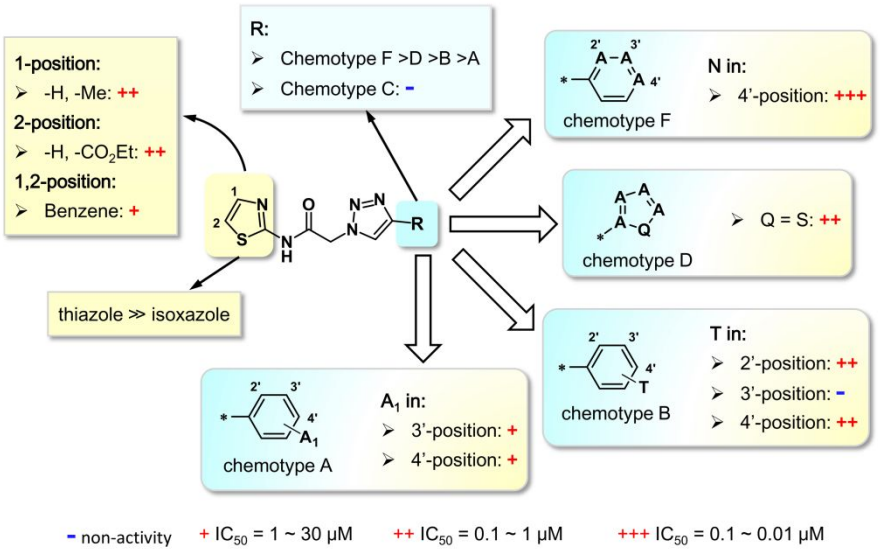

Figure 6. CAR and SAR of the discovered active anti-osteoporosis compounds. Blue background represents CAR and yellow represents SAR.

Compound 10a Prevents Bone Absorption *in vitro* and Has No Effect on Osteoblast Function. Compound **10a**, the most potent osteoclastogenesis inhibitor found so far, with IC_{50} = 2 nM, was selected for *in vivo* experiments and further studies of gene expression. Compound **10a** dose-dependently inhibits RANKL-induced osteoclast differentiation in BMMs (Figure 7A). The osteoclastogenesis-related genes (TRAcP, c-Fos, MMP-9, and NFATc1[31-33]) are highly expressed after RANKL treatment, but are significantly suppressed when compound **10a** is incubated with the BMMs (Figure 7B). It was shown in this way that compound **10a** inhibits osteoclast differentiation. The effect of compound **10a** on osteoclast function was further tested with a hydroxyapatite resorption assay (Figure 7C). In cells treated with **10a**, the area of osteoclast hydroxyapatite resorption is significantly reduced, compared to the

RANKL-treated group. Alizarin red staining reveals that compound **10a** exhibits no cytotoxicity and does not affect osteoblast differentiation and function in C3H10T1/2 cells (Figure 7D and Figure S5). All of the results from experiments *in vitro* indicate that compound **10a** should be subjected to further studies *in vivo*.

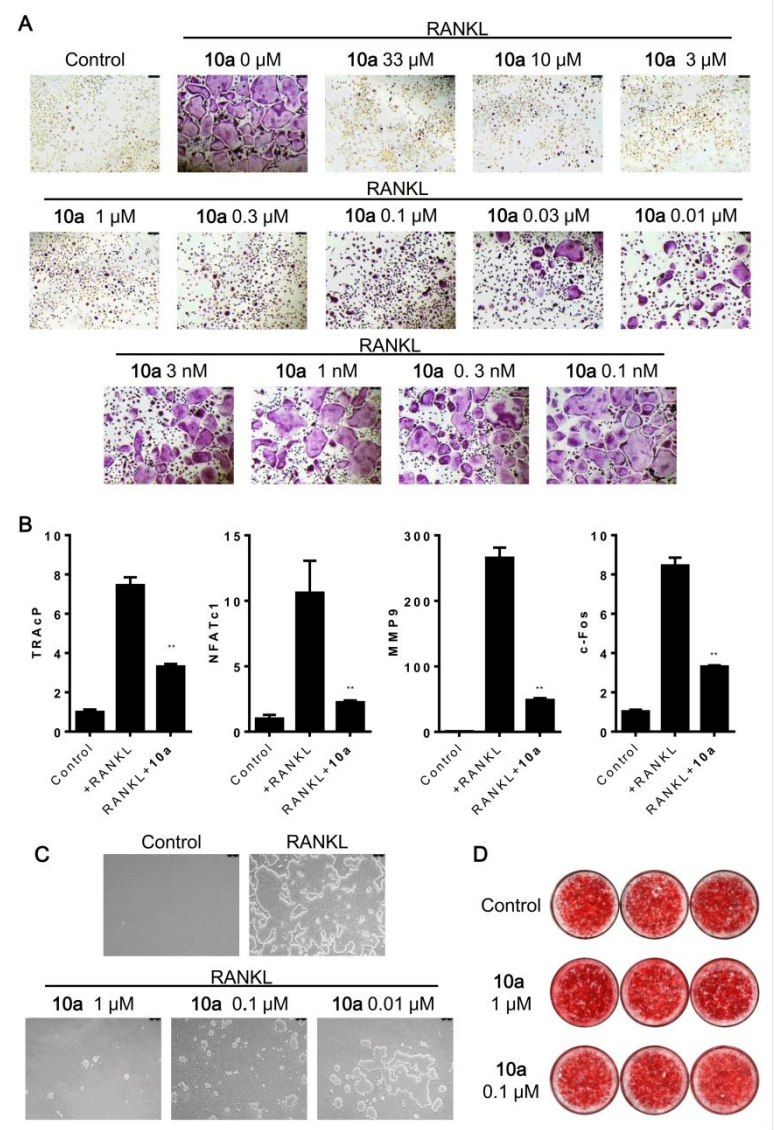

Figure 7. (**A**) Compound **10a** attenuates RANKL-induced osteoclastogenesis in a dose-dependent manner. (**B**) Compound **10a** (0.1 μM) down-regulates osteoclastogenic-related mRNA expression, including TRAcP, NFATc1, MMP9 and c-Fos. **, $P \leq 0.01$ compared with RANKL. (**C**) Representative image of bone resorption on hydroxyapatite-coated plates shows that **10a** can prevent bone resorption *in vitro*. (**D**) Determination of calcium deposition in differentiated osteoblasts by Alizarin red staining.

Compound 10a Prevents Bone Mass Loss *in vivo*. Studies of **10a** *in vivo* were made

in an ovariectomized (OVX) rat model, and Fosamax (sodium alendronate), a widely used and generally available drug was used as a positive control. Micro-CT results showed that compound **10a** significantly reduces bone mass loss (Figure 8A). Rats treated with **10a** show a loss of bone mineral density (BMD) of 8% on average. In the OVX and Fosamax-treated groups, the BMD loss in rats is on average, 19% and 3% respectively (Figure 8B). The level of collagen I C-terminal telopeptide (CTX-I), a bone turnover marker which is released during bone resorption was determined[32] and was found to have decreased in rats treated with **10a** (Figure 8D), compared to the OVX group. The concentrations of osteocalcin and procollagen-I N-terminal propeptide (PINP)[34-35] in the rats treated with **10a** are close to those in untreated rats (Figure 8D) and it was concluded that **10a** activates new bone formation. The RANKL level in serum was not affected by either **10a** or Fosamax. Routine blood tests indicate that rats treated with **10a** exhibit results similar to those of normal rats (sham group) (Figure S6). Compound **10a** has no organ toxicity (Figure S7) and, judging by the *in vivo* data, compound **10a** is a *bona fide* anti-osteoporosis agent.

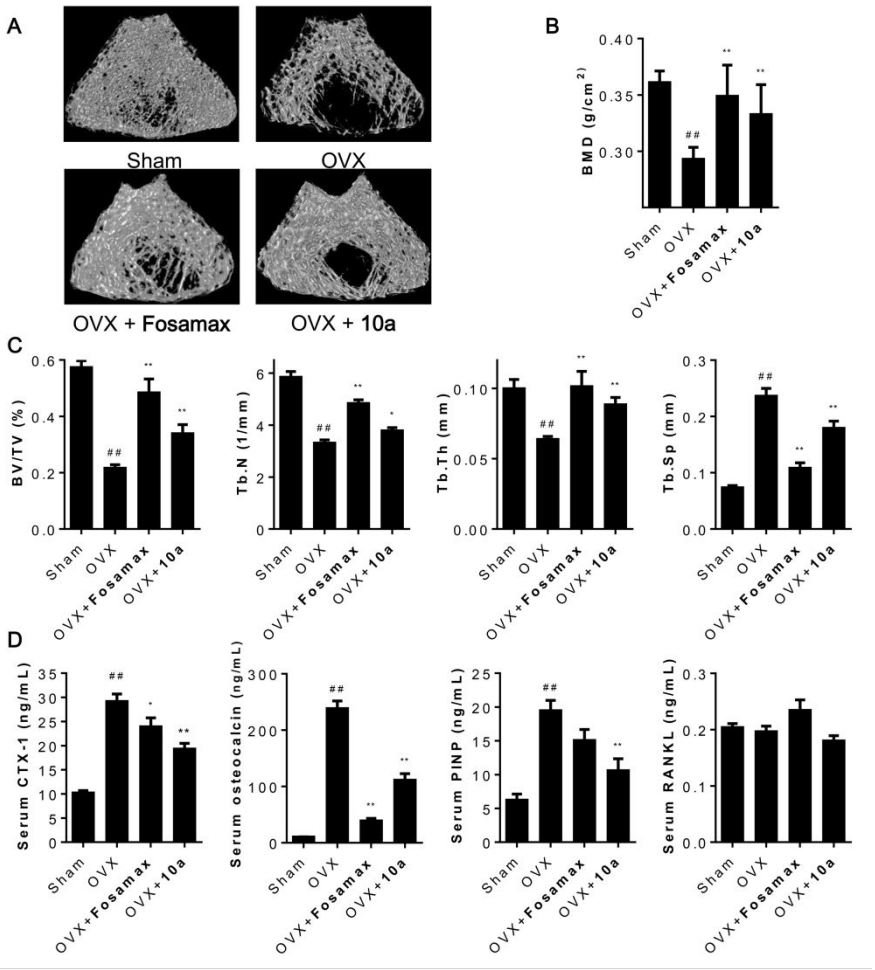

Figure 8. *In vivo* results for compound **10a**. (**A**) Micro-CT images of trabecular bone of femurs from sham-operated rats, ovariectomized rats (OVX) and rats treated with **10a**. (**B**) Femur BMD determined by dual-energy X-ray absorption. (**C**) Quantitative measurement of bone loss in femurs by micro-CT, BV/TV, bone volume as a fraction of total bone volume; Tb.N, Trabecular Number; Tb.Th, Trabecular Thickness; Tb.Sp, Trabecular Spacing. (**D**) Serum concentration of bone resorption and formation markers, CTX-I, osteocalcin, PINP and RANKL. Error bars are mean ± s.d. $^{\#\#}$, $P \leqslant 0.01$ compared with control; $^{\#\#\#}$, $P \leqslant 0.005$ compared with sham; *, $P \leqslant 0.05$ compared with OVX; **, $P \leqslant 0.01$ compared with OVX; ***, $P \leqslant 0.001$ compared with OVX.

CONCLUSIONS AND DISCUSSION

The chemotype-assembly approach combines fragments into a ligand-based drug discovery with superior performance. It is divided into three steps: (1) derivation of chemotypes and their assembly rules from a library of known compounds with a common target, a protein or a disease, (2) generation of compounds with affinity for a

target or disease based on given chemotype-assembled substructures, and (3) optimization of the identified leads using click chemistry, and *in vitro* and *in vivo* testing. In this way, we successfully assembled 69 anti-osteoporosis candidate compounds, confirmed 52 of these as anti-osteoporosis agents, and discovered 4 lead compounds with new scaffolds and nanomolar activity. The efficacy of the best compound (**10a**) was confirmed by *in vivo* experiments.

The chemotype-assembly approach allows getting the smallest active substructures for a target or diseases rationally and easily. By assembling the chemotypes through associated rules, the substructures can be easily obtained. These substructures can lead us to discover the hits of variety novel scaffolds with high hit rate. In this study, we discovered 7 novel anti-osteoporosis scaffold which are never reported before.

Click chemistry is a convenient technology with which to quickly generate a compound library. The triazole ring formed by click chemistry belongs to chemotype D, therefore, it can be used to optimize the candidates through the associated assembly rules. In this study, we successfully use click chemistry to optimize thiazole amide to a potent anti-osteoporosis lead compound (**10a**). Click chemistry also can be applied to discover *de novo* lead compounds according to the chemotype D assembly rules.

Compound **10a** significantly inhibits osteoclastogenesis *in vitro* and prevents bone loss *in vivo*. The serum PINP concentration of **10a** treated osteoporosis rats is closer to normal rats compare to Fosamax treated one. This result indicates compound **10a** may active new bone formation *in vivo*, since PINP is highly related to this function. Therefore, compound **10a** is a valuable lead for the development of potent anti-

osteoporosis drugs which can reduce the risk of fractures.

In conclusion, chemotype-assembly based drug discovery may offer a new approach to ligand-based drug discovery.

EXPERIMENTAL SECTION

Materials. Chemicals were purchased from Energy Chemical Co., Sigma-Aldrich Co. or Tokyo Chemical Industry Co. and utilized without further purification. Solvents were distilled prior to use. For *in vitro* and *in vivo* assay, α-Modified Minimal Essential Medium (α-MEM), Fetal bovine serum (FBS) and Phosphate buffered saline (PBS) were purchased from Gibco (Gibco, NY, USA). Tartrate resistant acid phosphatase (TRAcP) enzymatic activity was detected using the Leukocyte acid phosphatase staining kit (Sigma, St. Louis, MO, USA). Recombinant macrophage colony stimulating factor (M-CSF) was obtained from R&D Systems (Minneapolis, MN, USA). Glutathione S-transferase (GST)-rRANKL160–318 (GST-rRANKL) recombinant protein was expressed and purified as previously described[36]. Cell Counting Kit-8 (CCK-8) was obtained from Beyotime (Beyotime technology, China). Cell dissociation solution, dexamethasone, ascorbic acid, β-glycerol-phosphate and Alizarin red S was obtained from Sigma Aldrich (Sigma Aldrich, St Louis, MO, USA). Hydroxyapatite-coated 24 well plates were obtained from Corning (Corning, USA). TRIzol reagent was obtained from Invitrogen (Invitrogen, NY, USA). PrimeScript™ MixRT Master Mix reverse transcriptase kit and was TB Green™ premix EX Taq™ Ⅱ kit obtained from Takara (Takara Biotechnology, Kusatsu, Japan).

NMR spectroscopy and Mass spectrometry. ^{1}H-NMR and ^{13}C-NMR spectra were collected on a BRUKER 400 MHz spectrometer and were calibrated with tetramethylsilane. The NMR data are displayed as follows: chemical shifts (δ) are recorded as ppm, coupling constants (*J*) in hertz (Hz), integrity as the number of protons, and multiplicity as s (singlet), d (doublet), t (triplet), q (quartet), quintet, sextet, and m (multiplet). Mass spectra were obtained on a Shimadzu LCMS-2010EV utilizing the electron-spray ionization method (ESI-MS). Thin-layer chromatography (TLC) was carried out using plates coated with silica gel 60 F254, purchased from Merck. Column chromatography was performed using Merck silica gel 60 (70 - 230 mesh).

Animals. We performed all procedures on mice and rats with approval by the Sun Yat-sen University Institutional Animal Care and Use Committee. The C57BL/6 mice and female Sprague-Dawley (SD) rats were obtained from Guangdong Medical Lab Animal Center. Mice and rats were maintained in pressurized ventilated cages under conditions of repeated controlled illumination (12 h dark; 12 h light) with ad libitum access to sterilized water and food.

General procedure A for synthesis of compounds 1-5. Different substituted amino thiazoles and Et_3N was dissolved in CH_2Cl_2. Bromoacetyl bromide was added into the mixture by drop-wise at 0 ℃, and stirred at r.t. for 8h, followed by extraction with CH_2Cl_2. The extract was then washed with water, and brine, dried over Na_2SO_4, and evaporated *in vacuo*. The residue was purified by column chromatography to give products **1-5** as a solid. All compounds were found to have ≥95% purity by HPLC (Takara Biotechnology, Kusatsu, Japan)

2-Bromo-*N*-(thiazol-2-yl)acetamide (**1**). The general procedure A was applied with 2-amino-thiazole (100 mg, 1 mmol), Et_3N (218 mg, 2 mmol) and bromoacetyl bromide (301 mg, 1.5 mmol) to afford product **1** as a white solid (200 mg, 91.3%). ^{1}H-NMR (400 MHz, $CDCl_3$) δ: 7.53 (d, J = 4.0 Hz, 1H), 6.74 (d, J = 4.0 Hz, 1H), 5.21 (s, 2H).

2-Bromo-*N*-(4-methylthiazol-2-yl)acetamide (**2**). The general procedure A was applied with 2-amino-4-methylthiazole (114 mg, 1 mmol), Et_3N (218 mg, 2 mmol) and bromoacetyl bromide (301 mg, 1.5 mmol) to afford product **2** as an off-white solid (185 mg, 78.7%). ^{1}H-NMR (400 MHz, $CDCl_3$) δ: 6.82 (s, 1H), 5.22 (s, 2H), 2.28 (s, 3H).

Ethyl 2-(2-bromoacetamido)-4-methylthiazole-5-carboxylate (**3**). The general procedure A was applied with ethyl 2-amino-4-methylthiazole-5-carboxylate (186 mg, 1 mmol), Et_3N (218 mg, 2 mmol) and bromoacetyl bromide (301 mg, 1.5 mmol) to afford product **3** as a brown solid (177 mg, 57.7%). ^{1}H-NMR (400 MHz, $CDCl_3$) δ: 5.22 (s, 2H), 4.22 (q, J = 8.0 Hz, 2H), 2.53 (s, 3H), 1.26 (t, J = 8.0 Hz, 3H).

***N*-(Benzo[*d*]thiazol-2-yl)-2-bromoacetamide** (**4**). The general procedure A was applied with 2-benzothiazolamine (150 mg, 1 mmol), Et_3N (218 mg, 2 mmol) and bromoacetyl bromide (301 mg, 1.5 mmol) to afford product **4** as a yellow solid (120 mg, 44.3%). ^{1}H-NMR (400 MHz, $CDCl_3$) δ: 7.77 (d, J = 8.0 Hz, 1H), 7.74 (d, J = 8.0 Hz, 1H), 7.40 (t, J = 8.0 Hz, 1H), 7.28 (t, J = 8.0 Hz, 1H), 5.23 (s, 2H).

2-Bromo-*N*-(5-methylisoxazol-3-yl)acetamide (**5**). The general procedure A was applied with 5-methylisoxazol-3-amine (99 mg, 1 mmol), Et_3N (218 mg, 2 mmol) and bromoacetyl bromide (301 mg, 1.5 mmol) to afford product **5** as a white solid (195 mg, 89.9%). ^{1}H-NMR (400 MHz, $CDCl_3$) δ: 6.58 (s, 1H), 4.99 (s, 2H), 2.41 (s, 3H).

General procedure B for synthesis of compounds 6–10. The bromo-substituted compounds **1-5**, CuI and sodium azide was dissolved in DMSO, stirred at r.t. for 0.5 h. Then different alkyne compounds and DBU was added into the mixture, stirred at 70 ℃ for 8 h. The mixture was followed by extraction with EtOAc. The extract was then washed with water, and brine, dried over Na_2SO_4, and evaporated *in vacuo*. The residue was purified by column chromatography to give products **6-10** as a solid.

2-(4-(4-Methoxyphenyl)-1*H*-1,2,3-triazol-1-yl)-*N*-(thiazol-2-yl)acetamide (**6a**). The general procedure B was applied with compounds **1** (221 mg, 1 mmol), NaN_3 (130 mg, 2 mmol), CuI (19 mg, 0.1 mmol), 4-ethynylanisole (132 mg, 1 mmol) and DBU (304 mg, 2 mmol) to provide product **6a** as white solid (93 mg, 29.5%). ^{1}H-NMR (400 MHz, DMSO-*d6*) δ 12.58 (s, 1H), 7.54 (d, J = 4.0 Hz, 1H), 7.27-7.25 (m, 2H), 7.04-7.02 (m, 2H), 6.81 (s, 1H), 6.71 (d, J = 4.0 Hz, 1H), 5.53 (s, 2H), 3.88 (s, 3H). ^{13}C-NMR (100 MHz, DMSO-*d6*) δ 131.7, 119.4, 107.8, 100.0, 60.1, 45.4, 41.8, 33.6, 19.3. ESI-MS: 316.0 $[M+H]^+$.

2-(4-(4-Methoxyphenyl)-1*H*-1,2,3-triazol-1-yl)-*N*-(4-methylthiazol-2-yl)acetamide (**6b**). The general procedure B was applied with compounds **2** (233 mg, 1 mmol), NaN_3 (130 mg, 2 mmol), CuI (19 mg, 0.1 mmol), 4-ethynylanisole (132 mg, 1 mmol) and DBU (304 mg, 2 mmol) to provide product **6b** as white solid (142 mg, 43.2%). ^{1}H-NMR (400 MHz, DMSO-*d6*) δ 12.62 (s, 1H), 11.29 (s, 1H), 8.07-8.02 (m, 4H), 6.82 (s, 1H), 5.53 (s, 2H), 3.88 (s, 3H), 2.28 (s, 3H). ^{13}C-NMR (100 MHz, DMSO-*d6*) δ 166.4, 145.7, 135.6, 130.4, 129.2, 125.7, 124.8, 108.8, 52.6, 52.2, 17.3. ESI-MS: 330.0 $[M+H]^+$.

Ethyl 2-(2-(4-(4-methoxyphenyl)-1*H*-1,2,3-triazol-1-yl)-acetamido)-4-methylthiazole-5-carboxylate (**6c**). The general procedure B was applied with compounds **3** (301 mg, 1 mmol), NaN_3 (130 mg, 2 mmol), CuI (19 mg, 0.1 mmol), 4-ethynylanisole (132 mg, 1 mmol) and DBU (304 mg, 2 mmol) to provide product **6c** as white solid (93 mg, 29.5%). ^{1}H-NMR (400 MHz, DMSO-*d6*) δ 8.49 (s, 1H), 7.82-7.78 (m, 2H), 7.05-7.01 (m, 2H), 5.76 (s, 1H), 5.53 (s, 2H), 4.23 (q, J = 8.0 Hz, 2H), 2.57 (s, 3H), 1.26 (t, J = 8.0 Hz, 3H). ^{13}C-NMR (10 MHz, DMSO-*d6*) δ 166.4, 162.4, 159.8, 159.5, 156.6, 146.8, 127.0, 123.6, 122. 6, 114.8, 61.1, 55.6, 52.2, 17.5, 14.6. ESI-MS: 402.1 $[M+H]^+$.

***N*-(Benzo[*d*]thiazol-2-yl)-2-(4-(4-methoxyphenyl)-1*H*-1,2,3-triazol-1-yl)acetamide** (**6d**). The general procedure B was applied with compounds **4** (271 mg, 1 mmol), NaN_3 (130 mg, 2 mmol), CuI (19 mg, 0.1 mmol), 4-ethynylanisole (132 mg, 1 mmol) and DBU (304 mg, 2 mmol) to provide product **6d** as white solid (93 mg, 29.5%). ^{1}H-NMR (400 MHz, DMSO-*d6*) δ 8.53 (s, 1H), 8.00 (d, J = 8.0 Hz, 1H), 7.83-7.79 (m, 3H), 7.61 (d, J = 8.0 Hz, 1H), 7.47 (t, J = 8.0 Hz, 1H), 7.33 (t, J = 8.0 Hz, 1H), 7.04 (d, J = 8.0 Hz, 1H), 5.58 (s, 2H), 3.80 (s, 3H). ^{13}C-NMR (100 MHz, DMSO-*d6*) δ 159.5, 146.8, 127.0, 126.8, 124.3, 123.7, 122.6, 122.3, 121.2, 114.8, 55.6, 52.3. ESI-MS: 366.0 $[M+H]^+$.

2-(4-(4-Methoxyphenyl)-1*H*-1,2,3-triazol-1-yl)-*N*-(5-methylisoxazol-3-yl) acetamide (**6e**). The general procedure B was applied with compounds **5** (219 mg, 1 mmol), NaN_3 (130 mg, 2 mmol), CuI (19 mg, 0.1 mmol), 4-ethynylanisole (132 mg, 1 mmol) and DBU (304 mg, 2 mmol) to provide product **6e** as white solid (136 mg,

13.5%). ^{1}H-NMR (400 MHz, DMSO-*d6*) δ 11.49 (s, 1H), 8.45 (s, 1H), 7.79 (d, J = 8.0 Hz, 2H), 7.03 (d, J = 8.0 Hz, 2H), 6.59 (s, 1H), 5.40 (s, 2H), 3.80 (s, 3H), 2.38 (s, 3H). ^{13}C-NMR (100 MHz, DMSO-*d6*) δ 170.4, 165.2, 159.5, 158.1, 146.6, 127.0, 123.7, 122.6, 114.81, 96.6, 94.8, 55.6, 52.4, 29.7, 29.3, 12.6, 12.4. ESI-MS: 314.1 $[M+H]^+$.

2-(4-(3-Aminophenyl)-1*H*-1,2,3-triazol-1-yl)-*N*-(thiazol-2-yl)acetamide (**6f**). The general procedure B was applied with compounds **1** (221 mg, 1 mmol), NaN_3 (130 mg, 2 mmol), CuI (19 mg, 0.1 mmol), 3-ethynylaniline (117 mg, 1 mmol) and DBU (304 mg, 2 mmol) to provide product **6f** as white solid (65 mg, 21.7%). ^{1}H-NMR (400 MHz, DMSO-*d6*) δ 12.59 (s, 1H), 8.59 (s, 1H), 7.98 (d, J = 8.0 Hz, 1H), 7.93 (d, J = 8.0 Hz, 1H), 7.38 (t, J = 8.0 Hz, 1H), 7.27 (d, J = 4.0 Hz, 1H), 6.80 (d, J = 4.0 Hz, 1H), 5.53 (s, 2H), 4.25 (s, 2H). ^{13}C-NMR (100 MHz, DMSO-*d6*) δ 170.7, 170.3, 144.9, 128.1, 126.1, 123.3, 116.1, 116.2, 108.7, 61.0, 55.2, 21.2, 17.4. ESI-MS: 301.0 $[M+H]^+$.

2-(4-(3-Aminophenyl)-1*H*-1,2,3-triazol-1-yl)-*N*-(4-methylthiazol-2-yl)acetamide (**6g**). The general procedure B was applied with compounds **2** (233 mg, 1 mmol), NaN_3 (130 mg, 2 mmol), CuI (19 mg, 0.1 mmol), 3-ethynylaniline (117 mg, 1 mmol) and DBU (304 mg, 2 mmol) to provide product **6g** as white solid (75 mg, 23.9%). ^{1}H-NMR (400 MHz, DMSO-*d6*) δ 8.86 (s, 1H), 7.94-7.90 (m, 2H), 7.30 (t, J = 8.0 Hz, 2H), 6.81 (s, 1H), 5.50 (s, 2H), 2.28 (s, 3H). ^{13}C-NMR (100 MHz, DMSO-*d6*) δ 167.5, 130.5, 130.4, 125.6, 124.7, 108.8, 55.2, 52.2, 17.2. ESI-MS: 315.0 $[M+H]^+$.

2-(4-(3-Aminophenyl)-1*H*-1,2,3-triazol-1-yl)-*N*-(benzo[*d*]thiazol-2-yl)acetamide (**6h**). The general procedure B was applied with compounds **4** (271 mg, 1 mmol), NaN_3 (130 mg, 2 mmol), CuI (19 mg, 0.1 mmol), 3-ethynylaniline (117 mg, 1 mmol) and

DBU (304 mg, 2 mmol) to provide product **6h** as white solid (84 mg, 24.0%). ^{1}H-NMR (400 MHz, DMSO-*d6*) δ 12.68 (s, 1H), 8.60 (s, 1H), 8.01 (d, J = 8.0 Hz, 1H), 7.97 (d, J = 8.0 Hz, 1H), 7.53-7.44 (m, 3H), 7.32 (d, J = 8.0 Hz, 1H), 7.05 (d, J = 8.0 Hz, 1H), 6.88 (s, 1H), 5.58 (s, 2H), 4.45 (s, 2H). ^{13}C-NMR (100 MHz, DMSO-*d6*) δ 179.0, 168.0, 153.4, 148.3, 130.8, 127.7, 126.3, 118.5, 116.7, 114.3, 53.8. ESI-MS: 351.0 $[M+H]^+$.

2-(4-(4-Nitrophenyl)-1*H*-1,2,3-triazol-1-yl)-*N*-(thiazol-2-yl)acetamide (**7a**). The general procedure B was applied with compounds **1** (221 mg, 1 mmol), NaN_3 (130 mg, 2 mmol), CuI (19 mg, 0.1 mmol), 4-nitrophenylacetylene (147 mg, 1 mmol) and DBU (304 mg, 2 mmol) to provide product **7a** as white solid (121 mg, 36.7%). ^{1}H-NMR (400 MHz, DMSO-*d6*) δ 12.53 (s, 1H), 8.09 (d, J = 8.0 Hz, 2H), 7.95 (d, J = 8.0 Hz, 2H), 7.54 (d, J = 4.0 Hz, 1H), 6.81 (s, 1H), 6.71 (d, J = 4.0 Hz, 1H), 5.53 (s, 2H). ^{13}C-NMR (100 MHz, DMSO-*d6*) δ 148.5, 139.6, 129.3, 112.1, 96.2, 37.6, 28.3, 19.5. ESI-MS: 331.0 $[M+H]^+$.

***N*-(4-Methylthiazol-2-yl)-2-(4-(4-nitrophenyl)-1*H*-1,2,3-triazol-1-yl)acetamide** (**7b**). The general procedure B was applied with compounds **2** (233 mg, 1 mmol), NaN_3 (130 mg, 2 mmol), CuI (19 mg, 0.1 mmol), 4-nitrophenylacetylene (147 mg, 1 mmol) and DBU (304 mg, 2 mmol) to provide product **7b** as white solid (153 mg, 44.5%). ^{1}H-NMR (400 MHz, DMSO-*d6*) δ 12.63 (s, 1H), 8.89 (s, 1H), 8.36-8.32 (m, 2H), 8.19-8.15 (m, 2H), 6.82 (s, 1H), 5.56 (s, 2H), 2.29 (s, 3H). ^{13}C-NMR (100 MHz, DMSO-*d6*) δ 147.1, 144.9, 137.5, 126.5, 125.7, 124.9, 108.8, 52.3, 17.3. ESI-MS: 345.1 $[M+H]^+$.

Ethyl 4-methyl-2-(2-(4-(4-nitrophenyl)-1*H*-1,2,3-triazol-1-yl)acetamido)-thiazole-5-carboxylate (**7c**). The general procedure B was applied with compounds **3**

(221 mg, 1 mmol), NaN_3 (130 mg, 2 mmol), CuI (19 mg, 0.1 mmol), 4-nitrophenylacetylene (147 mg, 1 mmol) and DBU (304 mg, 2 mmol) to provide product **7c** as white solid (93 mg, 29.5%). ^{1}H-NMR (400 MHz, DMSO-*d6*) δ 8.87 (s, 1H), 8.35-8.33 (m, 2H), 8.18-8.16 (m, 2H), 7.10 (s, 1H), 5.56 (s, 2H), 4.22 (q, J = 8.0 Hz, 2H), 2.55 (s, 3H), 1.26 (t, J = 8.0 Hz, 3H). ^{13}C-NMR (100 MHz, DMSO-*d6*) δ 147.1, 144.9, 137.5, 126.4, 125.6, 124.9, 60.9, 52.8, 17.6, 14.6. ESI-MS: 417.0 $[M+H]^+$.

***N*-(Benzo[*d*]thiazol-2-yl)-2-(4-(4-nitrophenyl)-1*H*-1,2,3-triazol-1-yl)acetamide** (**7d**). The general procedure B was applied with compounds **4** (271 mg, 1 mmol), NaN_3 (130 mg, 2 mmol), CuI (19 mg, 0.1 mmol), 4-nitrophenylacetylene (147 mg, 1 mmol) and DBU (304 mg, 2 mmol) to provide product **7d** as white solid (93 mg, 29.5%). ^{1}H-NMR (400 MHz, DMSO-*d6*) δ 8.49 (s, 1H), 7.91 (d, J = 8.0 Hz, 2H), 7.76 (d, J = 8.0 Hz, 2H), 7.61 (d, J = 8.0 Hz, 1H), 7.36 (d, J = 8.0 Hz, 1H), 7.11 (t, J = 8.0 Hz, 1H), 6.96 (t, J = 8.0 Hz, 1H), 5.42 (s, 2H). ^{13}C-NMR (100 MHz, DMSO-*d6*) δ 179.9, 154.0, 130.9, 127.8, 126.5, 53.7, 50.0, 41.8, 34.5, 33.6, 33.4, 28.3. ESI-MS: 381.0 $[M+H]^+$.

***N*-(5-Methylisoxazol-3-yl)-2-(4-(4-nitrophenyl)-1*H*-1,2,3-triazol-1-yl)acetamide** (**7e**). The general procedure B was applied with compounds **5** (219 mg, 1 mmol), NaN_3 (130 mg, 2 mmol), CuI (19 mg, 0.1 mmol), 4-nitrophenylacetylene (147 mg, 1 mmol) and DBU (304 mg, 2 mmol) to provide product **7e** as white solid (89 mg, 27.1%). ^{1}H-NMR (400 MHz, DMSO-*d6*) δ 11.54 (s, 1H), 8.87 (s, 1H), 8.34 (d, J = 8.0 Hz, 2H), 8.16 (d, J = 8.0 Hz, 2H), 6.60 (s, 1H), 5.50 (s, 2H), 2.39 (s, 3H). ^{13}C-NMR (100 MHz, DMSO-*d6*) δ 194.5, 170.5, 165.0, 158.1, 147.1, 144.8, 137.5, 126.4, 125.7, 124.9, 96.6, 52.6, 21.2, 12.6. ESI-MS: 329.0 $[M+H]^+$.

2-(4-(4-Chlorophenyl)-1*H*-1,2,3-triazol-1-yl)-*N*-(thiazol-2-yl)acetamide (7f). The general procedure B was applied with compounds **1** (221 mg, 1 mmol), NaN_3 (130 mg, 2 mmol), CuI (19 mg, 0.1 mmol), 4-chlorophenylacetylene (136 mg, 1 mmol) and DBU (304 mg, 2 mmol) to provide product **7f** as white solid (78 mg, 24.5%). ^{1}H-NMR (400 MHz, DMSO-*d6*) δ 12.71 (s, 1H), 8.68 (s, 1H), 7.92 (d, J = 8.0 Hz, 2H), 7.54 (d, J = 8.0 Hz, 2H), 7.53 (d, J = 4.0 Hz, 1H), 7.29 (d, J = 4.0 Hz, 1H), 5.53 (s, 2H). ^{13}C-NMR (100 MHz, DMSO-*d6*) δ 165.1, 158.0, 145.7, 139.1, 138.2, 132.8, 130.0, 129.5, 127.3, 123.9, 114.6, 52.1. ESI-MS: 320.1 $[M+H]^+$.

2-(4-(4-Chlorophenyl)-1*H*-1,2,3-triazol-1-yl)-*N*-(4-methylthiazol-2-yl)acetamide (7g). The general procedure B was applied with compounds **2** (233 mg, 1 mmol), NaN_3 (130 mg, 2 mmol), CuI (19 mg, 0.1 mmol), 4-chlorophenylacetylene (136 mg, 1 mmol) and DBU (304 mg, 2 mmol) to provide product **7g** as yellow solid (53 mg, 15.9%). ^{1}H-NMR (400 MHz, DMSO-*d6*) δ 12.51 (s, 1H), 8.61 (s, 1H), 7.91-7.89 (m, 2H), 7.52-7.50 (m, 2H), 6.79 (s, 1H), 5.50 (s, 2H), 1.98 (s, 3H). ^{13}C-NMR (100 MHz, DMSO-*d6*) δ 170.8, 145.7, 132.9, 129.9, 129.4, 127.3, 123.8, 108.6, 60.2, 55.2, 21.0, 14.3. ESI-MS: 334.1 $[M+H]^+$.

Ethyl 2-(2-(4-(4-chlorophenyl)-1*H*-1,2,3-triazol-1-yl)acetamido)-4-methylthiazole-5-carboxylate (7h). The general procedure B was applied with compounds **3** (221 mg, 1 mmol), NaN_3 (130 mg, 2 mmol), CuI (19 mg, 0.1 mmol), 4-chlorophenylacetylene (136 mg, 1 mmol) and DBU (304 mg, 2 mmol) to provide product **7h** as white solid (166 mg, 41.0%). ^{1}H-NMR (400 MHz, DMSO-*d6*) δ 12.92 (s, 1H), 8.68 (s, 1H), 7.90 (d, J = 8.0 Hz, 2H), 7.62 (d, J = 8.0 Hz, 2H), 5.53 (s, 2H),

4.21 (q, *J* = 8.0 Hz, 2H), 2.55 (s, 3H), 1.25 (t, *J* = 8.0 Hz, 3H). ^{13}C-NMR (100 MHz, DMSO-*d6*) δ 162.9, 116.1, 148.0, 121.1, 134.3, 128.5, 129.4, 60.9, 59.3, 16.4, 14.5. ESI-MS: 406.0 $[M+H]^+$.

***N*-(Benzo[*d*]thiazol-2-yl)-2-(4-(4-chlorophenyl)-1*H*-1,2,3-triazol-1-yl)acetamide** (**7i**). The general procedure B was applied with compounds **4** (271 mg, 1 mmol), NaN_3 (130 mg, 2 mmol), CuI (19 mg, 0.1 mmol), 4-chlorophenylacetylene (136 mg, 1 mmol) and DBU (304 mg, 2 mmol) to provide product **7i** as white solid (125 mg, 33.9%). ^{1}H-NMR (400 MHz, DMSO-*d6*) δ 8.60 (s, 1H), 7.92 (d, *J* = 8.0 Hz, 2H), 7.63 (d, *J* = 8.0 Hz, 1H), 7.52 (d, *J* = 8.0 Hz, 2H), 7.41 (d, *J* = 8.0 Hz, 1H), 7.17 (t, *J* = 8.0 Hz, 1H), 6.99 (t, *J* = 8.0 Hz, 1H), 5.14 (s, 2H). ^{13}C-NMR (100 MHz, DMSO-*d6*) δ 145.2, 132.4, 130.6, 129.4, 127.2, 124.6, 123.7, 121.1, 120.8, 55.8. ESI-MS: 370.0 $[M+H]^+$.

2-(4-(4-Chlorophenyl)-1*H*-1,2,3-triazol-1-yl)-*N*-(5-methylisoxazol-3-yl)acetamide (**7j**). The general procedure B was applied with compounds **5** (219 mg, 1 mmol), NaN_3 (130 mg, 2 mmol), CuI (19 mg, 0.1 mmol), 4-chlorophenylacetylene (136 mg, 1 mmol) and DBU (304 mg, 2 mmol) to provide product **7j** as white solid (142 mg, 44.8%). ^{1}H-NMR (400 MHz, DMSO-*d6*) δ 11.58 (s, 1H), 8.71 (s, 1H), 7.99 (d, *J* = 8.0 Hz, 2H), 7.60 (d, *J* = 8.0 Hz, 2H), 6.65 (s, 1H), 5.52 (s, 2H), 2.45 (s, 3H). ^{13}C-NMR (100 MHz, DMSO-*d6*) δ 170.5, 165.2, 158.1, 145.6, 132.8, 130.1, 130.0, 129.5, 127.3, 123.9, 96.6, 94.8, 52.5, 12.6. ESI-MS: 318.1 $[M+H]^+$.

2-(4-(4-Cyanophenyl)-1*H*-1,2,3-triazol-1-yl)-*N*-(thiazol-2-yl)acetamide (**7k**). The general procedure B was applied with compounds **1** (221 mg, 1 mmol), NaN_3 (130 mg, 2 mmol), CuI (19 mg, 0.1 mmol), 4-ethynylbenzonitrile (127 mg, 1 mmol) and DBU

(304 mg, 2 mmol) to provide product **7k** as white solid (90 mg, 29.03%). ^{1}H-NMR (400 MHz, DMSO-*d6*) δ 12.70 (s, 1H), 8.83 (s, 1H), 8.09 (d, J = 8.0 Hz, 2H), 7.84 (d, J = 8.0 Hz, 2H), 7.52 (d, J = 4.0 Hz, 1H), 7.25 (d, J = 4.0 Hz, 1H), 5.57 (s, 2H). ^{13}C-NMR (100 MHz, DMSO-*d6*) δ 168.8, 145.9, 126.7, 125.6, 122.7, 118.2, 116.4, 116.2, 79.4, 60.2, 52.1, 21.2, 14.5. ESI-MS: 311.2 $[M+H]^+$.

Ethyl 2-(2-(4-(4-cyanophenyl)-1*H*-1,2,3-triazol-1-yl)acetamido)-4-methylthiazole-5-carboxylate (**7l**). The general procedure B was applied with compounds **3** (221 mg, 1 mmol), NaN_3 (130 mg, 2 mmol), CuI (19 mg, 0.1 mmol), 4-ethynylbenzonitrile (127 mg, 1 mmol) and DBU (304 mg, 2 mmol) to provide product **7l** as white solid (128 mg, 32.3%). ^{1}H-NMR (400 MHz, DMSO-*d6*) δ 12.71 (s, 1H), 8.82 (s, 1H), 8.29 (d, J = 8.0 Hz, 2H), 7.91 (d, J = 8.0 Hz, 2H), 5.58 (s, 2H). 4.22 (q, J = 8.0 Hz, 2H), 2.53 (s, 3H), 1.26 (t, J = 8.0 Hz, 3H). ^{13}C-NMR (100 MHz, DMSO-*d6*) δ 170.9, 162.9, 156.5, 134.8, 125.9, 125,3, 121.7, 118.6, 116.1, 61.0, 59.0, 144.9, 17.6, 14.7. ESI-MS: 397.1 $[M+H]^+$.

***N*-(Benzo[*d*]thiazol-2-yl)-2-(4-(4-cyanophenyl)-1*H*-1,2,3-triazol-1-yl)acetamide** (**7m**). The general procedure B was applied with compounds **4** (271 mg, 1 mmol), NaN_3 (130 mg, 2 mmol), CuI (19 mg, 0.1 mmol), 4-ethynylbenzonitrile (127 mg, 1 mmol) and DBU (304 mg, 2 mmol) to provide product **7m** as white solid (158 mg, 51.0%). ^{1}H-NMR (400 MHz, DMSO-*d6*) δ 12.98 (s, 1H), 8.86 (s, 1H), 8.10 (d, J = 8.0 Hz, 2H), 8.01 (d, J = 8.0 Hz, 1H), 7.95 (d, J = 8.0 Hz, 2H), 7.80 (d, J = 8.0 Hz, 1H), 7.47 (t, J = 8.0 Hz, 1H), 7.34 (t, J = 8.0 Hz, 1H), 5.66 (s, 2H). ^{13}C-NMR (100 MHz, DMSO-*d6*) δ 145.3, 135.5, 133.5, 126.8, 126.2, 125.3, 124.3, 122.4, 119.3, 110.7. ESI-MS: 360.0

$[M+H]^+$.

2-(4-(4-Cyanophenyl)-1*H*-1,2,3-triazol-1-yl)-*N*-(5-methylisoxazol-3-yl)acetamide (**7n**). The general procedure B was applied with compounds **5** (219 mg, 1 mmol), NaN_3 (130 mg, 2 mmol), CuI (19 mg, 0.1 mmol), 4-ethynylbenzonitrile (127 mg, 1 mmol) and DBU (304 mg, 2 mmol) to provide product **7n** as white solid (144 mg, 46.8%). ^{1}H-NMR (400 MHz, DMSO-*d6*) δ 11.54 (s, 1H), 8.80 (s, 1H), 8.08 (d, J = 8.0 Hz, 2H), 7.94 (d, J = 8.0 Hz, 2H), 6.60 (s, 1H), 5.48 (s, 2H), 2.39 (s, 3H). ^{13}C-NMR (100 MHz, DMSO-*d6*) δ 170.5, 165.1, 158.1, 145.2, 135.6, 133.5, 126.2, 125.3, 119.3, 110.6, 96.6, 52.6, 12.6. ESI-MS: 309.2 $[M+H]^+$.

2-(4-(4-Fluorophenyl)-1*H*-1,2,3-triazol-1-yl)-*N*-(thiazol-2-yl)acetamide (**7o**). The general procedure B was applied with compounds **1** (221 mg, 1 mmol), NaN_3 (130 mg, 2 mmol), CuI (19 mg, 0.1 mmol), 4-fluorophenylacetylene (120 mg, 1 mmol) and DBU (304 mg, 2 mmol) to provide product **7o** as white solid (130 mg, 42.9%). ^{1}H-NMR (400 MHz, DMSO-*d6*) δ 12.71 (s, 1H), 8.61 (s, 1H), 7.93 (d, J = 8.0 Hz, 2H), 7.52 (d, J = 4.0 Hz, 1H), 7.31 (d, J = 8.0 Hz, 2H), 7.28 (d, J = 4.0 Hz, 1H), 5.53 (s, 2H).. ^{13}C-NMR (100 MHz, DMSO-*d6*) δ 170.8, 145.9, 127.7, 127.6, 123.5, 116.5, 116.2, 79.4, 60.2, 52.1, 21.2, 14.6. ESI-MS: 304.0 $[M+H]^+$.

2-(4-(4-Fluorophenyl)-1*H*-1,2,3-triazol-1-yl)-*N*-(4-methylthiazol-2-yl)acetamide (**7p**). The general procedure B was applied with compounds **2** (233 mg, 1 mmol), NaN_3 (130 mg, 2 mmol), CuI (19 mg, 0.1 mmol), 4-fluorophenylacetylene (120 mg, 1 mmol) and DBU (304 mg, 2 mmol) to provide product **7p** as white solid (66 mg, 20.8%). ^{1}H-NMR (400 MHz, DMSO-*d6*) δ 12.63 (s, 1H), 8.86 (s, 1H), 7.92 (t, J = 8.0 Hz, 2H),

7.30 (t, *J* = 8.0 Hz, 2H), 6.81 (s, 1H), 5.50 (s, 2H), 1.99 (s, 3H). ^{13}C-NMR (100 MHz, DMSO-*d6*) δ 145.9, 127.7, 127.6, 123.4, 116.4, 116.2, 108.7, 60.2, 55.3, 21.2, 17.2, 14.6. ESI-MS: 318.1 $[M+H]^+$.

Ethyl 2-(2-(4-(4-fluorophenyl)-1*H*-1,2,3-triazol-1-yl)acetamido)-4-methylthiazole-5-carboxylate (**7q**). The general procedure B was applied with compounds **3** (221 mg, 1 mmol), NaN_3 (130 mg, 2 mmol), CuI (19 mg, 0.1 mmol), 4-fluorophenylacetylene (120 mg, 1 mmol) and DBU (304 mg, 2 mmol) to provide product **7q** as white solid (111 mg, 28.5%). ^{1}H-NMR (400 MHz, DMSO-*d6*) δ 13.08 (s, 1H), 8.61 (s, 1H), 7.92 (d, *J* = 8.0 Hz, 2H), 7.33 (d, *J* = 8.0 Hz, 2H), 5.58 (s, 2H), 4.24 (q, *J* = 8.0 Hz, 2H), 2.58 (s, 3H), 1.27 (t, *J* = 8.0 Hz, 3H). ^{13}C-NMR (100 MHz, DMSO-*d6*) δ 163.5, 162.4, 161.1, 146.0, 127.7, 127.6, 127.6, 123.5, 116.5, 116.3, 61.1, 52.2, 17.5, 14.6. ESI-MS: 390.2 $[M+H]^+$.

***N*-(Benzo[*d*]thiazol-2-yl)-2-(4-(4-fluorophenyl)-1*H*-1,2,3-triazol-1-yl)acetamide** (**7r**). The general procedure B was applied with compounds **4** (271 mg, 1 mmol), NaN_3 (130 mg, 2 mmol), CuI (19 mg, 0.1 mmol), 4-fluorophenylacetylene (120 mg, 1 mmol) and DBU (304 mg, 2 mmol) to provide product **7r** as white solid (104 mg, 29.5%). ^{1}H-NMR (400 MHz, DMSO-*d6*) δ 12.95 (s, 1H), 8.65 (s, 1H), 8.01 (d, *J* = 8.0 Hz, 1H), 7.93 (d, *J* = 8.0 Hz, 2H), 7.80 (d, *J* = 8.0 Hz, 1H), 7.47 (t, *J* = 8.0 Hz, 1H), 7.36-7.30 (m, 3H), 5.62 (s, 2H). ^{13}C-NMR (100 MHz, DMSO-*d6*) δ 166.2, 163.5, 161.1, 157.8, 146.0, 127.7, 127.7, 126.8, 124.3, 123.5, 122.4, 121.3, 116.5, 116.3, 52.3, 31.8, 30.3. ESI-MS: 354.1 $[M+H]^+$.

2-(4-(4-Fluorophenyl)-1*H*-1,2,3-triazol-1-yl)-N-(5-methylisoxazol-3-

yl)acetamide (**7s**). The general procedure B was applied with compounds **5** (219 mg, 1 mmol), NaN_3 (130 mg, 2 mmol), CuI (19 mg, 0.1 mmol), 4-fluorophenylacetylene (120 mg, 1 mmol) and DBU (304 mg, 2 mmol) to provide product **7s** as white solid (74 mg, 24.6%). ^{1}H-NMR (400 MHz, DMSO-*d6*) δ 11.51 (s, 1H), 8.58 (s, 1H), 7.94 (d, J = 8.0 Hz, 2H), 7.31 (d, J = 8.0 Hz, 2H), 6.60 (s, 1H), 5.44 (s, 2H), 2.39 (s, 3H). ^{13}C-NMR (100 MHz, DMSO-*d6*) δ 170.5, 165.2, 158.1, 145.9, 127.7, 127.6, 123.4, 116.5, 116.2, 96.6, 94.8, 52.4, 12.6. ESI-MS: 302.2 $[M+H]^+$.

2-(4-(2-Chlorophenyl)-1*H*-1,2,3-triazol-1-yl)-*N*-(thiazol-2-yl)acetamide (**7t**). The general procedure B was applied with compounds **1** (221 mg, 1 mmol), NaN_3 (130 mg, 2 mmol), CuI (19 mg, 0.1 mmol), 2-chlorophenylacetylene (136 mg, 1 mmol) and DBU (304 mg, 2 mmol) to provide product **7t** as white solid (162 mg, 53.0%). ^{1}H-NMR (400 MHz, DMSO-*d6*) δ 12.64 (s, 1H), 8.77 (s, 1H), 8.14 (d, J = 4.0 Hz, 1H), 7.60 (d, J = 4.0 Hz, 1H), 7.53 – 7.28 (m, 4H), 5.58 (s, 2H). ^{13}C-NMR (100 MHz, DMSO-*d6*) δ 165.2, 143.0, 130.8, 130.7, 129.9, 129.9, 129.5, 128.1, 126.5, 52.1. ESI-MS: 320.2 $[M+H]^+$.

2-(4-(2-Chlorophenyl)-1*H*-1,2,3-triazol-1-yl)-*N*-(4-methylthiazol-2-yl)acetamide (**7u**). The general procedure B was applied with compounds **2** (233 mg, 1 mmol), NaN_3 (130 mg, 2 mmol), CuI (19 mg, 0.1 mmol), 2-chlorophenylacetylene (136 mg, 1 mmol) and DBU (304 mg, 2 mmol) to provide product **7u** as white solid (65 mg, 19.5%). ^{1}H-NMR (400 MHz, DMSO-*d6*) δ 12.61 (s, 1H), 8.76 (s, 1H), 8.14 (d, J = 8.0 Hz, 1H), 7.60 (d, J = 8.0 Hz, 1H), 7.49 (t, J = 8.0 Hz, 1H), 7.41 (t, J = 8.0 Hz, 1H), 6.82 (s, 1H), 5.55 (s, 2H), 2.29 (s, 3H). ^{13}C-NMR (100 MHz, DMSO-*d6*) δ 142.9, 130.8, 130.7, 129.9,

129.9, 129.5, 128.1, 126.5, 108.8, 56.5, 52.1, 19.0, 17.3. ESI-MS: 334.2 $[M+H]^+$.

Ethyl 2-(2-(4-(2-chlorophenyl)-1*H*-1,2,3-triazol-1-yl)acetamido)-4-methylthiazole-5-carboxylate (**7v**). The general procedure B was applied with compounds **3** (221 mg, 1 mmol), NaN_3 (130 mg, 2 mmol), CuI (19 mg, 0.1 mmol), 2-chlorophenylacetylene (136 mg, 1 mmol) and DBU (304 mg, 2 mmol) to provide product **7v** as white solid (98 mg, 24.3%). ^{1}H-NMR (400 MHz, DMSO-*d6*) δ 13.07 (s, 1H), 8.77 (s, 1H), 8.14 (d, J = 8.0 Hz, 1H), 7.60 (d, J = 8.0 Hz, 1H), 7.49 (t, J = 8.0 Hz, 1H), 7.41 (t, J = 8.0 Hz, 1H), 5.62 (s, 2H), 4.23 (q, J = 8.0 Hz, 2H), 2.59 (s, 3H), 1.25 (t, J = 8.0 Hz, 3H). ^{13}C-NMR (100 MHz, DMSO-*d6*) δ 190.4, 162.4, 143.0, 130.8, 130.7, 130.0, 129.9, 129.5, 128.1, 126.5, 61.1, 56.5, 19.0, 17.5, 14.6. ESI-MS: 405.2 $[M+H]^+$.

***N*-(Benzo[*d*]thiazol-2-yl)-2-(4-(2-chlorophenyl)-1*H*-1,2,3-triazol-1-yl)acetamide** (**7w**). The general procedure B was applied with compounds **4** (271 mg, 1 mmol), NaN_3 (130 mg, 2 mmol), CuI (19 mg, 0.1 mmol), 2-chlorophenylacetylene (136 mg, 1 mmol) and DBU (304 mg, 2 mmol) to provide product **7w** as white solid (99 mg, 26.8%). ^{1}H-NMR (400 MHz, DMSO-*d6*) δ 12.95 (s, 1H), 8.81 (s, 1H), 8.16 (d, J = 8.0 Hz, 1H), 8.01 (d, J = 8.0 Hz, 1H), 7.80 (d, J = 8.0 Hz, 1H), 7.61 (d, J = 8.0 Hz, 1H), 7.52-7.33 (m, 4H), 5.66 (s, 2H). ^{13}C-NMR (100 MHz, DMSO-*d6*) δ 143.0, 130.8, 130.7, 130.0, 129.9, 129.5, 128.1, 126.8, 126.6, 125.9, 124.3, 122.3, 121.3, 118.2, 52.3, 49.2, 37.0, 29.5. ESI-MS: 370.2 $[M+H]^+$.

2-(4-(2-Chlorophenyl)-1*H*-1,2,3-triazol-1-yl)-*N*-(5-methylisoxazol-3-yl)acetamide (**7x**). The general procedure B was applied with compounds **5** (219 mg, 1 mmol), NaN_3 (130 mg, 2 mmol), CuI (19 mg, 0.1 mmol), 2-chlorophenylacetylene

(136 mg, 1 mmol) and DBU (304 mg, 2 mmol) to provide product **7x** as white solid (103 mg, 32.5%). ^{1}H-NMR (400 MHz, DMSO-*d6*) δ 11.49 (s, 1H), 8.72 (s, 1H), 8.13 (d, J = 8.0 Hz, 1H), 7.59 (d, J = 8.0 Hz, 1H), 7.48 (t, J = 8.0 Hz, 1H), 7.41 (t, J = 8.0 Hz, 1H), 6.60 (s, 1H), 5.48 (s, 2H), 2.39 (s, 3H). ^{13}C-NMR (100 MHz, DMSO-*d6*) δ 170.4, 165.2, 158.1, 142.9, 130.8, 130.7, 129.9, 129.6, 128.1, 126.5, 96.6, 52.4, 12.6. ESI-MS: 318.2 $[M+H]^{+}$.

2-(4-(3-Chlorophenyl)-1*H*-1,2,3-triazol-1-yl)-*N*-(thiazol-2-yl)acetamide (**7y**). The general procedure B was applied with compounds **1** (221 mg, 1 mmol), NaN_3 (130 mg, 2 mmol), CuI (19 mg, 0.1 mmol), 3-chlorophenylacetylene (147 mg, 1 mmol) and DBU (304 mg, 2 mmol) to provide product **7y** as white solid (156 mg, 48.9%). ^{1}H-NMR (400 MHz, DMSO-*d6*) δ 12.60 (s, 1H), 8.86 (s, 1H), 8.75 – 8.58 (m, 3H), 7.86 (d, J = 4.0 Hz, 2H), 6.79 (d, J = 8.0 Hz, 1H), 5.55 (s, 2H). ^{13}C-NMR (100 MHz, DMSO-*d6*) δ 165.3, 165.2, 150.9, 144.5, 138.2, 125.6, 120.2, 120.1, 119.9, 108.6, 52.5, 17.3. ESI-MS: 320.2 $[M+H]^{+}$.

2-(4-(3-Chlorophenyl)-1*H*-1,2,3-triazol-1-yl)-*N*-(5-methylisoxazol-3-yl)acetamide (**7z**). The general procedure B was applied with compounds **5** (219 mg, 1 mmol), NaN_3 (130 mg, 2 mmol), CuI (19 mg, 0.1 mmol), 3-chlorophenylacetylene (147 mg, 1 mmol) and DBU (304 mg, 2 mmol) to provide product **7z** as white solid (169 mg, 53.3%). ^{1}H-NMR (400 MHz, DMSO-*d6*) δ 11.50 (s, 1H), 8.69 (s, 1H), 7.94 (s, 1H), 7.85 (d, J = 8.0 Hz, 1H), 7.51 (t, J = 8.0 Hz, 1H), 7.41 (d, J = 8.0 Hz, 2H), 6.59 (s, 1H), 5.45 (s, 2H), 2.39 (s, 3H). ^{13}C-NMR (100 MHz, DMSO-*d6*) δ 170.5, 165.1, 158.1, 145.4, 134.2, 133.2, 131.4, 128.2, 125.2, 124.3, 124.2, 96.6, 52.5, 12.6. ESI-MS:

318.2 $[M+H]^+$.

Methyl 4-(1-(2-((4-methylthiazol-2-yl)amino)-2-oxoethyl)-1*H*-1,2,3-triazol-4-yl)benzoate (**8a**). The general procedure B was applied with compounds **2** (233 mg, 1 mmol), NaN_3 (130 mg, 2 mmol), CuI (19 mg, 0.1 mmol), methyl 4-ethynylbenzoate (160 mg, 1 mmol) and DBU (304 mg, 2 mmol) to provide product **8a** as white solid (123 mg, 34.5%). ^{1}H-NMR (400 MHz, DMSO-*d6*) δ 12.59 (s, 1H), 8.49 (s, 1H), 7.82-7.78 (m, 2H), 7.05-6.81 (m, 2H), 6.81 (s, 1H), 5.48 (s, 2H), 3.80 (s, 3H), 2.28 (s, 3H). ^{13}C-NMR (100 MHz, DMSO-*d6*) δ 159.5, 146.751, 127.0, 123.7, 122.6, 114.8, 108.8, 100.0, 55.6, 52.0, 17.3. ESI-MS: 357.9 $[M+H]^+$.

Methyl 4-(1-(2-(benzo[*d*]thiazol-2-ylamino)-2-oxoethyl)-1*H*-1,2,3-triazol-4-yl) benzoate (**8b**). The general procedure B was applied with compounds **4** (271 mg, 1 mmol), NaN_3 (130 mg, 2 mmol), CuI (19 mg, 0.1 mmol), methyl 4-ethynylbenzoate (160 mg, 1 mmol) and DBU (304 mg, 2 mmol) to provide product **8b** as white solid (65 mg, 16.1%). ^{1}H-NMR (400 MHz, DMSO-*d6*) δ 12.96 (s, 1H), 8.80 (s, 1H), 8.07-8.04 (m, 4H), 8.00 (d, J = 8.0 Hz, 1H), 7.80 (d, J = 8.0 Hz, 1H), 7.47 (t, J = 8.0 Hz, 1H), 7.34 (t, J = 8.0 Hz, 1H), 5.64 (s, 2H), 1.23 (s, 3H). ^{13}C-NMR (100 MHz, DMSO-*d6*) δ 180.0, 154.0, 130.9, 127.8, 126.5, 53.7, 50.0, 41.8, 34.5, 33.6, 33.4, 28.3. ESI-MS: 393.9 $[M+H]^+$.

Methyl 4-(1-(2-((5-methylisoxazol-3-yl)amino)-2-oxoethyl)-1*H*-1,2,3-triazol-4-yl) benzoate (**8c**). The general procedure B was applied with compounds **5** (219 mg, 1 mmol), NaN_3 (130 mg, 2 mmol), CuI (19 mg, 0.1 mmol), 4-ethynylbenzoate (160 mg, 1 mmol) and DBU (304 mg, 2 mmol) to provide product **8c** as white solid (128 mg,

37.5%). ^{1}H-NMR (400 MHz, DMSO-*d6*) δ 11.59 (s, 1H), 8.81 (s, 1H), 8.14-8.08 (m, 4H), 6.66 (s, 1H), 5.54 (s, 2H), 3.95 (s, 3H), 2.46 (s, 3H). ^{13}C-NMR (100 MHz, DMSO-*d6*) δ 170.5, 166.4, 165.1, 158.1, 145.7, 135.6, 130.4, 129.2, 125.7, 125.7, 124.8, 96.6, 61.2, 52.6, 12.6. ESI-MS: 341.2 $[M+H]^+$.

4-(1-(2-((4-Methylthiazol-2-yl)amino)-2-oxoethyl)-1H-1,2,3-triazol-4-yl)benzoic acid (**8d**). The general procedure B was applied with compounds **2** (233 mg, 1 mmol), NaN_3 (130 mg, 2 mmol), CuI (19 mg, 0.1 mmol), 4-ethynylbenzoic acid (146 mg, 1 mmol) and DBU (304 mg, 2 mmol) to provide product **8d** as white solid (89 mg, 25.9%). ^{1}H-NMR (400 MHz, DMSO-*d6*) δ 12.78 (s, 1H), 8.72 (s, 1H), 8.04-7.99 (m, 4H), 6.82 (s, 1H), 5.53 (s, 2H), 2.28 (s, 3H). ^{13}C-NMR (100 MHz, DMSO-*d6*) δ 167.5, 130.5, 130.4, 125.6, 124.7, 108.7, 55.2, 52.2, 17.2. ESI-MS: 344.0 $[M+H]^+$.

2-(4-(4-Ethynylphenyl)-1*H*-1,2,3-triazol-1-yl)-*N*-(thiazol-2-yl)acetamide (**8e**). The general procedure B was applied with compounds **1** (221 mg, 1 mmol), NaN_3 (130 mg, 2 mmol), CuI (19 mg, 0.1 mmol), 1,4-diethynylbenzene (126 mg, 1 mmol) and DBU (304 mg, 2 mmol) to provide product **8e** as white solid (180 mg, 58.3%). ^{1}H-NMR (400 MHz, DMSO-*d6*) δ 12.69 (s, 1H), 8.69 (s, 1H), 7.91 (d, J = 8.0 Hz, 2H), 7.58 (d, J = 8.0 Hz, 2H), 7.52 (d, J = 4.0 Hz, 1H), 7.28 (d, J = 4.0 Hz, 1H), 4.25 (s, 1H), 5.55 (s, 2H). ^{13}C-NMR (100 MHz, DMSO-*d6*) δ 165.1, 146.0, 132.8, 131.5, 125.8, 124.16, 121.5, 114.6, 83.8, 81.9, 52.1. ESI-MS: 310.0 $[M+H]^+$.

2-(4-(4-Ethynylphenyl)-1*H*-1,2,3-triazol-1-yl)-*N*-(5-methylisoxazol-3-yl)acetamide (**8f**). The general procedure B was applied with compounds **5** (219 mg, 1 mmol), NaN_3 (130 mg, 2 mmol), CuI (19 mg, 0.1 mmol), 1,4-diethynylbenzene (126

mg, 1 mmol) and DBU (304 mg, 2 mmol) to provide product **8f** as white solid (75 mg, 24.4%). ^{1}H-NMR (400 MHz, DMSO-*d6*) δ 11.50 (s, 1H), 8.65 (s, 1H), 7.90 (d, J = 8.0 Hz, 2H), 7.56 (d, J = 8.0 Hz, 2H), 6.59 (s, 1H), 5.46 (s, 2H), 4.24 (s, 1H), 2.39 (s, 3H). ^{13}C-NMR (100 MHz, DMSO-*d6*) δ 170.4, 165.2, 159.5, 158.1, 146.6, 127.0, 123.7, 122.6, 114.8, 96.6, 94.8, 55.6, 52.4, 29.7, 29.3, 12.6, 12.4. ESI-MS: 308.2 $[M+H]^+$.

***N*-(Thiazol-2-yl)-2-(4-(thiophen-2-yl)-1*H*-1,2,3-triazol-1-yl)acetamide** (**9a**). The general procedure B was applied with compounds **1** (221 mg, 1 mmol), NaN_3 (130 mg, 2 mmol), CuI (19 mg, 0.1 mmol), 2-ethynylthiophene (108 mg, 1 mmol) and DBU (304 mg, 2 mmol) to provide product **9a** as white solid (95 mg, 32.6%). ^{1}H-NMR (400 MHz, DMSO-*d6*) δ 12.70 (s, 1H), 8.53 (s, 1H), 7.55 (d, J = 4.0 Hz, 1H), 7.52 (d, J = 4.0 Hz, 1H), 7.47 (d, J = 4.0 Hz, 1H), 7.28 (d, J = 4.0 Hz, 1H), 7.15 (t, J = 4.0 Hz, 1H), 5.52 (s, 2H). ^{13}C-NMR (100 MHz, DMSO-*d6*) δ 142.2, 128.4, 125.9, 124.7, 122.9, 114.62, 60.2, 52.1, 14.6. ESI-MS: 292.0 $[M+H]^+$.

***N*-(4-Methylthiazol-2-yl)-2-(4-(thiophen-2-yl)-1*H*-1,2,3-triazol-1-yl)acetamide** (**9b**). The general procedure B was applied with compounds **2** (233 mg, 1 mmol), NaN_3 (130 mg, 2 mmol), CuI (19 mg, 0.1 mmol), 2-ethynylthiophene (108 mg, 1 mmol) and DBU (304 mg, 2 mmol) to provide product **9b** as light yellow solid (44 mg, 14.4%). ^{1}H-NMR (400 MHz, Acetone-*d6*) δ 12.60 (s, 1H), 8.22 (s, 1H), 7.72-7.70 (m, 1H), 7.46-7.42 (m, 2H), 6.59 (s, 1H), 5.49 (s, 2H), 3.18 (s, 3H). ^{13}C-NMR (100 MHz, Acetone-*d6*) δ 126.4, 125.8, 122.1, 121.7, 120.5, 108.1, 66.3, 59.7, 29.5, 29.3, 29.1, 29.0, 28.8, 28.6, 28.4, 19.9, 16.2, 13.6. ESI-MS: 305.9 $[M+H]^+$.

Ethyl 4-methyl-2-(2-(4-(thiophen-2-yl)-1*H*-1,2,3-triazol-1-

yl)acetamido)thiazole-5-carboxylate (**9c**). The general procedure B was applied with compounds **3** (221 mg, 1 mmol), NaN_3 (130 mg, 2 mmol), CuI (19 mg, 0.1 mmol), 2-ethynylthiophene (108 mg, 1 mmol) and DBU (304 mg, 2 mmol) to provide product **9c** as white solid (93 mg, 29.5%). ^{1}H-NMR (400 MHz, DMSO-*d6*) δ 12.70 (s, 1H), 8.53 (s, 1H), 7.56-7.45 (m, 1H), 7.28 (d, J = 4.0 Hz, 1H), 7.15 (t, J = 4.0 Hz, 1H), 5.52 (s, 2H), 4.03 (q, J = 8.0 Hz, 2H), 1.99 (s, 3H), 1.22 (t, J = 8.0 Hz, 3H). ^{13}C-NMR (100 MHz, DMSO-*d6*) δ 179.0, 167.7, 142.2, 128.4, 126.7, 125.9, 124.7, 122.9, 114.6, 60.2, 52.1, 40.6, 29.5, 14.6. ESI-MS: 377.9 $[M+H]^+$.

***N*-(Benzo[*d*]thiazol-2-yl)-2-(4-(thiophen-2-yl)-1*H*-1,2,3-triazol-1-yl)acetamide** (**9d**). The general procedure B was applied with compounds **4** (271 mg, 1 mmol), NaN_3 (130 mg, 2 mmol), CuI (19 mg, 0.1 mmol), 2-ethynylthiophene (108 mg, 1 mmol) and DBU (304 mg, 2 mmol) to provide product **9d** as yellow solid (87 mg, 25.5%). ^{1}H-NMR (400 MHz, DMSO-*d6*) δ 12.93 (s, 1H), 8.56 (s, 1H), 8.01 (d, J = 8.0 Hz, 1H), 7.80 (d, J = 8.0 Hz, 1H), 7.56 (d, J = 8.0 Hz, 1H), 7.51-7.42 (m, 2H), 7.35 (t, J = 8.0 Hz, 1H), 7.16 (t, J = 8.0 Hz, 1H), 5.59 (s, 2H). ^{13}C-NMR (100 MHz, DMSO-*d6*) δ 142.2, 133.3, 128.4, 126.8, 125.9, 124.7, 124.3, 122.9, 122.3, 52.3. ESI-MS: 342.0 $[M+H]^+$.

***N*-(5-Methylisoxazol-3-yl)-2-(4-(thiophen-2-yl)-1*H*-1,2,3-triazol-1-yl)acetamide** (**9e**). The general procedure B was applied with compounds **5** (219 mg, 1 mmol), NaN_3 (130 mg, 2 mmol), CuI (19 mg, 0.1 mmol), 2-ethynylthiophene (108 mg, 1 mmol) and DBU (304 mg, 2 mmol) to provide product **9e** as white solid (65 mg, 22.5%). ^{1}H-NMR (400 MHz, DMSO-*d6*) δ 11.50 (s, 1H), 8.49 (s, 1H), 7.54 (d, J = 4.0 Hz, 1H), 7.46 (d, J = 4.0 Hz, 1H), 7.14 (t, J = 4.0 Hz, 1H), 6.59 (s, 1H), 5.42 (s, 2H), 2.38 (s, 3H). ^{13}C-

NMR (101 MHz, DMSO) δ 170.46, 165.10, 158.07, 142.09, 133.35, 128.40, 125.87, 124.61, 122.86, 96.61, 52.42, 12.62. ESI-MS: 290.0 $[M+H]^+$.

2-(4-(Pyridin-4-yl)-1*H*-1,2,3-triazol-1-yl)-*N*-(thiazol-2-yl)acetamide (**10a**). The general procedure B was applied with compounds **1** (221 mg, 1 mmol), NaN_3 (130 mg, 2 mmol), CuI (19 mg, 0.1 mmol), 4-ethynylpyridine (103 mg, 1 mmol) and DBU (304 mg, 2 mmol) to provide product **10a** as brown solid (104 mg, 36.4%). ^{1}H-NMR (400 MHz, DMSO-*d6*) δ 12.74 (s, 1H), 8.87 (s, 1H), 8.67 (bs, 2H), 7.86 (d, J = 4.0 Hz, 2H), 7.53 (d, J = 4.0 Hz, 1H), 7.28 (d, J = 4.0 Hz, 1H), 5.60 (s, 2H). ^{13}C-NMR (100 MHz, DMSO-*d6*) δ 165.0, 158.0, 150.8, 144.5, 138.2, 125.6, 120.1, 114.6, 52.2. ESI-MS: 287.0 $[M+H]^+$. The Purity was determined by high-performance liquid chromatography (HPLC, SHIMADZU LC-20AT, Japan). Compounds were dissolved at a concentration of 0.5 mg/mL in methanol. Then, 150 μL of the sample was injected into a Agilent XDB-C18 HPLC column (4.6 × 250 mm; particle size, 5 μm) and chromatographed using a gradient of water/MeCN from 90:10 to 50:50 for 15 min at a flow rate of 250 μL/min. UV absorption was detected from 100 to 950 nm using a diode array detector.

***N*-(4-Methylthiazol-2-yl)-2-(4-(pyridin-4-yl)-1*H*-1,2,3-triazol-1-yl)acetamide** (**10b**). The general procedure B was applied with compounds **2** (233 mg, 1 mmol), NaN_3 (130 mg, 2 mmol), CuI (19 mg, 0.1 mmol), 4-ethynylpyridine (103 mg, 1 mmol) and DBU (304 mg, 2 mmol) to provide product **10b** as dark red solid (106 mg, 35.3%). ^{1}H-NMR (400 MHz, DMSO-*d6*) δ 12.62 (s, 1H), 8.86 (s, 1H), 8.75 – 8.61 (m, 2H), 7.86 (s, 1H), 6.78 (s, 1H), 5.55 (s, 2H), 2.28 (s, 3H). ^{13}C-NMR (100 MHz, DMSO-*d6*)

δ 165.3, 150.9, 144.5, 138.2, 125.6, 120.1, 108.6, 52.5, 17.3. ESI-MS: 301.0 $[M+H]^+$.

Ethyl 4-methyl-2-(2-(4-(pyridin-4-yl)-1*H*-1,2,3-triazol-1-yl)acetamido)thiazole-5-carboxylate (**10c**). The general procedure B was applied with compounds **3** (221 mg, 1 mmol), NaN_3 (130 mg, 2 mmol), CuI (19 mg, 0.1 mmol), 4-ethynylpyridine (103 mg, 1 mmol) and DBU (304 mg, 2 mmol) to provide product **10c** as brown solid (110 mg, 29.6%). ^{1}H-NMR (400 MHz, DMSO-*d6*) δ 8.85 (s, 1H), 8.84-8.69 (m, 2H), 7.88 (d, J = 8.0 Hz, 2H), 5.56 (s, 2H), 4.20 (q, J = 8.0 Hz, 2H), 2.55 (s, 3H), 1.27 (t, J = 8.0 Hz, 3H). ^{13}C-NMR (100 MHz, DMSO-*d6*) δ 162.6, 150.8, 146.3, 144.5, 138.2, 125.6, 60.9, 53.0, 28.7, 17.6, 14.76. ESI-MS: 373.2 $[M+H]^+$.

***N*-(Benzo[*d*]thiazol-2-yl)-2-(4-(pyridin-4-yl)-1*H*-1,2,3-triazol-1-yl)acetamide** (**10d**). The general procedure B was applied with compounds **4** (271 mg, 1 mmol), NaN_3 (130 mg, 2 mmol), CuI (19 mg, 0.1 mmol), 4-ethynylpyridine (103 mg, 1 mmol) and DBU (304 mg, 2 mmol) to provide product **10d** as red solid (105 mg, 31.3%). ^{1}H-NMR (400 MHz, DMSO-*d6*) δ 12.94 (s, 1H), 8.89 (s, 1H), 8.71 (bs, 2H), 8.00 (d, J = 8.0 Hz, 1H), 7.90 (bs, 2H), 7.80 (d, J = 8.0 Hz, 1H), 7.47 (t, J = 8.0 Hz, 1H), 7.33 (t, J = 8.0 Hz, 1H), 5.66 (s, 2H). ^{13}C-NMR (100 MHz, DMSO-*d6*) δ 144.6, 131.9, 126.7, 125.7, 124.3, 122.4, 121.1, 100.0, 85.0, 52.5. ESI-MS: 337.1 $[M+H]^+$.

***N*-(5-Methylisoxazol-3-yl)-2-(4-(pyridin-4-yl)-1*H*-1,2,3-triazol-1-yl)acetamide** (**10e**). The general procedure B was applied with compounds **5** (219 mg, 1 mmol), NaN_3 (130 mg, 2 mmol), CuI (19 mg, 0.1 mmol), 4-ethynylpyridine (103 mg, 1 mmol) and DBU (304 mg, 2 mmol) to provide product **10e** as brown solid (171 mg, 60.2%). ^{1}H-NMR (400 MHz, DMSO-*d6*) δ 11.53 (s, 1H), 8.83 (s, 1H), 8.73 (bs, 2H), 7.87 (bs, 2H),

6.59 (s, 1H), 5.49 (s, 2H), 2.39 (s, 3H). ^{13}C-NMR (100 MHz, DMSO-*d6*) δ 170.5, 165.0, 158.1, 150.8, 144.4, 125.6, 96.6, 52.6, 12.6. ESI-MS: 285.2 $[M+H]^+$.

Cell culture. C3H10T1/2 cells were obtained from America Type Culture Collection (Mannassasa, VA, USA) and maintained in complete α-MEM (α-MEM, 10% heat inactivated FBS, 2 mM L-glutamine and 100 U/mL penicillin/streptomycin). Cultured the cells in 5% CO_2 at 37 °C.

***In vitro* osteoclastogenesis assay.** Osteoclastogenesis assay using previous reported method.BMMs were isolated from six-week-old C57BL/6 mice by flushing the marrow from the femur and tibia. Cells were then cultured in α-MEM supplemented with 10% FBS, 2 mM L-glutamine, 100 U/ml penicillin, and 100 μg/mL streptomycin (complete medium), in the presence of M-CSF (30 ng/mL). To generate osteoclasts, BMMs were plated in 96-well plates at a density of 6×10^3 cells/well in the presence of M-CSF (30 ng/mL) overnight. The following day, cells were then stimulated with complete medium containing M-CSF and GST-rRANKL (100 ng/mL) in the presence or absence of compounds with different concentrations every 2 days until osteoclasts formed. After 5 days, cells were fixed with 4% paraformaldehyde and then stained for TRAcP enzymatic activity using a leucocyte acid phosphatase staining kit, following the manufacturer's procedures. TRAcP-positive multinucleated cells (>3 nuclei) were counted as osteoclast-like (OCL) cells.

Cytotoxicity assay. A CCK-8 assay was used to determine cell viability. BMMs and C3H10T1/2 cells in the logarithmic growth phase were cultured in 96-well plates with 6×10^3 cells in each well and incubated for 24 h. The cells were then treated with

DMSO vehicle or with different concentrations of compounds ranging from 0.1 μM to 100 μM for 48 h or 72 h. Then, 10 μL CCK-8 was added to each well, wells were incubated at 37 ℃ for 30 min, and absorbance was then measured at 450 nm using a microplate reader (Thermo, USA).

Hydroxyapatite resorption assay. BMMs (1×10^5 cells/well) were cultured onto 6-well collagen-coated plates and stimulated with GST-rRANKL and M-CSF (30 ng/mL) until mature osteoclasts formed. Cells were gently harvested using cell dissociation solution and consistent numbers of mature osteoclasts were seeded into hydroxyapatite-coated 24 well plates. Mature osteoclasts were incubated in medium containing GST-rRANKL and M-CSF with or without compounds 7t, 9c and 10a. After 48 h, wells were bleached to remove cells, followed by image acquisition for the measurement of resorbed areas using a Leica inverted microscope (Leica, Germany). The percentage of surface resorbed was analyzed using Image J software (NIH, Bethesda, USA).

Real time polymerase chain reaction (real-time PCR). For Real-Time PCR, BMMs were seeded in a 6-well plate at a density of 1×10^5 cells per well and then cultured in complete α-MEM with M-CSF (30 ng/mL), GST-rRANKL (100 ng/mL), and with or without compound **10a** at 0.1 μM for 5 days. For RT–qPCR analysis, total cellular RNA was extracted cultured cells with TRIzol reagent, following the manufacturer's protocol. Reverse transcription was performed using PrimeScript™ MixRT Master Mix reverse transcriptase kit, according to the manufacturer's specifications. RT-qPCR was performed using TB Green™ premix EX Taq™ Ⅱ kit with 1 μL reverse transcriptase for 40 cycles of 95 °C for 10 s, 56 °C for 10 s and 72 °C

for 30 s. Primer sequences are as follows:

		sequences
NFATc1	forward	5'-CAACGCCCTGACCACCGATAG-3'
	reverse	5'-GGCTGCCTTCCGTCTCATAGT-3'
c-Fos	forward	5'-CCAGTCAAGAGCATCAGCAA-3'
	reverse	5'-AAGTAGTGCAGCCCGGAGTA-3'
MMP9	forward	5'-CCTACTCTGCCTGCACCACTAAA-3'
	reverse	5'-CTGCTTGCCCAGGAAGACGAA-3'
TRAP	forward	5'-GGCTATGTGCTGAG-3'
	reverse	5'-GGAGGCTGGTCTTA-3'

Alizarin red staining assay. Alizarin red assay using previous reported method. C3H10T1/2 cells were respectively seeded at a density of 5×10^4 cells/cm^2 on 24-well plate and maintained in complete growth media for 24 hours (α-MEM with 10% FBS, 100 U/mL penicillin and 100 mg/mL streptomycin) in a humidified atmosphere of 5% CO_2 at 37 °C, then the cells were induced with osteogenic medium (OS media, the growth medium with 5% FBS, 10^{-7} M dexamethasone, 50 μM ascorbic acid and 10 mM β-glycerol-phosphate) with or without compound **10a**. After 14 days, cells were washed with PBS twice and then fixed with 4.0% formaldehyde. The cells were stained with 0.1% Alizarin red solution (pH 4.4) for 5 min at room temperature and rinsed with deionized water twice.

Ovariectomized (OVX) rat model and compound 10a treatment. Thirty two 6-month-old female SD rats were randomly divided into 4 groups. After anesthesia, 8 of them were subjected to a sham-operated experiment (as Sham group), where the rest of them were all subjected to bilateral ovariectomy. After 3 months, the OVX rat were separated into three groups and were individually oral administration with physiological saline (as OVX group), 1 mg/kg/d Fosamax (as OVX+Fosamax group)

and 10 mg/kg/d compound **10a** (as OVX+**10a** group) for another 3 months. The weight of rats was recorded every month. After 3 months, the rats were harvested and the serum, heart, liver, spleen, lung, kidney, thymus and femurs were all collected and subjected to subsequent analysis.

Bone mineral density analysis. The right femurs of rats were applied for analysis. After fixation with 4% paraformaldehyde, bone mineral density (BMD) was measured by dual-energy-X-ray absorption (DXA; DCS-600, Aloka, Tokyo, Japan). Moreover, the Micro-CT analysis was also scanned on Inveon PET/CT (Siemens, Germany). Regions of interest (ROIs) were defined for trabecular and cortical parameters. The trabecular ROI extended from 1 mm proximally to the end of the distal growth plate over 1 mm toward the diaphysis. The resulting two-dimensional images of trabecular bone in relative cross-sections were shown in grayscale. Trabecular bone parameters were measured including bone volume/tissue volume (BV/TV), trabecular number (Tb.N), trabecular thickness (Tb.Th), and trabecular separation (Tb.Sp).

Statistics. The mean ± s.d. was performed to express numerical data and histograms. Two-tailed Student's t-test was performed between two groups and a difference was considered statistically significant with $P < 0.05$.

ASSOCIATED CONTENT

Supporting Infromation

Tables S1~S5, Figures S1~S7, NMR spectra of compound **10a** and HPLC trace of **10a**. Molecular formula strings and anti-osteoclatogenesis data.

AUTHOR INFORMATION

Corresponding Authors

*For J. X. E-mail: junxu@biochemomes.com

*For Q. G. E-mail: guqiong@mail.sysu.edu.cn

Author contributions

C.Z. and D.H. contributed equally to this work.

C.Z., D.H., Q.G. and J.X. designed the overall study. C.Z. performed the *in silico* experiments. C.Z., Y.X. and S.S. performed the chemical experiments. D.H. and R.L. performed biological experiments. Q.G. and J.X. supervise the overall study. C.Z., Q.G. and J.X. wrote and edit the manuscript.

Notes

The authors declare no competing financial interest.

ACKNOWLEDGMENTS

This work was funded in part of Natural Science Foundation of China (81473138, 81573310, 81803361), GD-NSF (2018A030310143), GD Frontier & Key Techn. Innovation Program (2015B010109004) and GD Provincial Key Laboratory of Construction Foundation (2017B030314030).

ABBREVIATIONS

NMR, nuclear magnetic resonance; LBDD, ligand-based drug discovery; QSAR, quantitative structure-activity relationship; LXRβ, liver X receptor-β; DSGA, *de novo* substructure generation algorithm; SCA, scaffold-based classification approach; SERM, selective estrogen-receptor modulator; SARM, selective androgen-receptor modulator;

BPs, bisphosphonates; D2R agonist dopamine receptor D2 agonist; DPP-IV inhibitor, dipeptidyl peptidase-4 inhibitor; RANKL, activator of nuclear factor-kappa B ligand; SAR, structure-activity relationship; CAR, chemotype-activity relationship; BMMs, bone marrow-derived macrophages; TRAcP, tartrate resistant acid phosphatase; NFATc1, nuclear factor of activated T-cells, cytoplasmic 1; MMP9, matrix metallopeptidase 9; OVX, ovariectomized; BMD, bone mineral density; CTX-I, C-terminal telopeptide; PINP, procollagen-I N-terminal propeptide.

REFERENCES

1. Walters, W. P.; Namchuk, M., Designing Screens: How to Make Your Hits a Hit. *Nature reviews. Drug discovery* **2003,** *2* (4), 259-266.

2. Gini, G., Qsar: What Else? *Methods Mol Biol* **2018,** *1800* 79-105.

3. Hull, R. D.; Fluder, E. M.; Singh, S. B.; Nachbar, R. B.; Kearsley, S. K.; Sheridan, R. P., Chemical Similarity Searches Using Latent Semantic Structural Indexing (Lassi) and Comparison to Toposim. *J Med Chem* **2001,** *44* (8), 1185-1191.

4. Peng, H.; Liu, Z.; Yan, X.; Ren, J.; Xu, J., A De Novo Substructure Generation Algorithm for Identifying the Privileged Chemical Fragments of Liver X Receptorbeta Agonists. *Sci Rep* **2017,** *7* (1), 11121.

5. Moffat, J. G.; Vincent, F.; Lee, J. A.; Eder, J.; Prunotto, M., Opportunities and Challenges in Phenotypic Drug Discovery: An Industry Perspective. *Nature reviews. Drug discovery* **2017,** *16* (8), 531-543.

6. Erlanson, D. A.; Fesik, S. W.; Hubbard, R. E.; Jahnke, W.; Jhoti, H., Twenty Years On: The Impact of Fragments on Drug Discovery. *Nat Rev Drug Discov* **2016,** *15* (9), 605-619.

7. Karasik, D.; Rivadeneira, F.; Johnson, M. L., The Genetics of Bone Mass and Susceptibility to Bone Diseases. *Nat Rev Rheumatol* **2016,** *12* (8), 496.

8. Allen, J. G.; Fotsch, C.; Babij, P., Emerging Targets in Osteoporosis Disease Modification. *J Med Chem* **2010,** *53* (11), 4332-4353.

9. Black, D. M.; Rosen, C. J., Clinical Practice. Postmenopausal Osteoporosis. *N Engl J Med* **2016,** *374* (3), 254-262.

10. Whitaker, M.; Guo, J.; Kehoe, T.; Benson, G., Bisphosphonates for Osteoporosis--Where Do We Go from Here? *N Engl J Med* **2012,** *366* (22), 2048-2051.

11. Drake, M. T.; Clarke, B. L.; Oursler, M. J.; Khosla, S., Cathepsin K Inhibitors for Osteoporosis: Biology, Potential Clinical Utility, and Lessons Learned. *Endocr Rev* **2017,** *38* (4), 325-350.

12. Sage, A. P.; Lu, J.; Atti, E.; Tetradis, S.; Ascenzi, M. G.; Adams, D. J.; Demer, L. L.; Tintut, Y., Hyperlipidemia Induces Resistance to Pth Bone Anabolism in Mice Via Oxidized Lipids. *J Bone Miner Res*

2011, *26* (6), 1197-1206.

13. Modi, A.; Sajjan, S.; Gandhi, S., Challenges in Implementing and Maintaining Osteoporosis Therapy. *Int J Womens Health* **2014,** *6* 759-769.

14. Congreve, M.; Carr, R.; Murray, C.; Jhoti, H., A 'Rule of Three' for Fragment-Based Lead Discovery? *Drug Discov Today* **2003,** *8* (19), 876-877.

15. Xu, J., A New Approach to Finding Natural Chemical Structure Classes. *J Med Chem* **2002,** *45* (24), 5311-5320.

16. Chen, H.; Zhou, X.; Wang, A.; Zheng, Y.; Gao, Y.; Zhou, J., Evolutions in Fragment-Based Drug Design: The Deconstruction-Reconstruction Approach. *Drug Discov Today* **2015,** *20* (1), 105-113.

17. Over, B.; Wetzel, S.; Grutter, C.; Nakai, Y.; Renner, S.; Rauh, D.; Waldmann, H., Natural-Product-Derived Fragments for Fragment-Based Ligand Discovery. *Nat Chem* **2013,** *5* (1), 21-28.

18. Palacios, S.; Silverman, S. L.; de Villiers, T. J.; Levine, A. B.; Goemaere, S.; Brown, J. P.; De Cicco Nardone, F.; Williams, R.; Hines, T. L.; Mirkin, S.; Chines, A. A.; Bazedoxifene Study, G., A 7-Year Randomized, Placebo-Controlled Trial Assessing the Long-Term Efficacy and Safety of Bazedoxifene in Postmenopausal Women with Osteoporosis: Effects on Bone Density and Fracture. *Menopause* **2015,** *22* (8), 806-813.

19. Basaria, S.; Collins, L.; Dillon, E. L.; Orwoll, K.; Storer, T. W.; Miciek, R.; Ulloor, J.; Zhang, A.; Eder, R.; Zientek, H.; Gordon, G.; Kazmi, S.; Sheffield-Moore, M.; Bhasin, S., The Safety, Pharmacokinetics, and Effects of Lgd-4033, a Novel Nonsteroidal Oral, Selective Androgen Receptor Modulator, in Healthy Young Men. *J Gerontol A Biol Sci Med Sci* **2013,** *68* (1), 87-95.

20. Falgueyret, J. P.; Desmarais, S.; Oballa, R.; Black, W. C.; Cromlish, W.; Khougaz, K.; Lamontagne, S.; Masse, F.; Riendeau, D.; Toulmond, S.; Percival, M. D., Lysosomotropism of Basic Cathepsin K Inhibitors Contributes to Increased Cellular Potencies against Off-Target Cathepsins and Reduced Functional Selectivity. *J Med Chem* **2005,** *48* (24), 7535-7543.

21. Hanai, Y.; Tokuda, H.; Takai, S.; Harada, A.; Ohta, T.; Kozawa, O., Minodronate Suppresses Prostaglandin F2alpha-Induced Vascular Endothelial Growth Factor Synthesis in Osteoblasts. *Horm Metab Res* **2006,** *38* (3), 152-158.

22. Di Somma, C.; Colao, A.; Di Sarno, A.; Klain, M.; Landi, M. L.; Facciolli, G.; Pivonello, R.; Panza, N.; Salvatore, M.; Lombardi, G., Bone Marker and Bone Density Responses to Dopamine Agonist Therapy in Hyperprolactinemic Males. *J Clin Endocrinol Metab* **1998,** *83* (3), 807-813.

23. Marquis, R. W.; Ru, Y.; LoCastro, S. M.; Zeng, J.; Yamashita, D. S.; Oh, H. J.; Erhard, K. F.; Davis, L. D.; Tomaszek, T. A.; Tew, D.; Salyers, K.; Proksch, J.; Ward, K.; Smith, B.; Levy, M.; Cummings, M. D.; Haltiwanger, R. C.; Trescher, G.; Wang, B.; Hemling, M. E.; Quinn, C. J.; Cheng, H. Y.; Lin, F.; Smith, W. W.; Janson, C. A.; Zhao, B.; McQueney, M. S.; D'Alessio, K.; Lee, C. P.; Marzulli, A.; Dodds, R. A.; Blake, S.; Hwang, S. M.; James, I. E.; Gress, C. J.; Bradley, B. R.; Lark, M. W.; Gowen, M.; Veber, D. F., Azepanone-Based Inhibitors of Human and Rat Cathepsin K. *J Med Chem* **2001,** *44* (9), 1380-1395.

24. Schennetten, F.; Leissa, H., [Therapy of the Postmenopausal Osteoporosis Using Methyltestosterone Plus Ergocalciferol or Methylandrostenedione]. *Med Welt* **1976,** *27* (9), 444-445.

25. Ucar, A.; Abaci, A.; Pirgon, O.; Dundar, B.; Tutunculer, F.; Catli, G.; Anik, A.; Kilinc Ugurlu, A.; Buyukgebiz, A., A Synopsis of Current Practice in the Diagnosis and Management of Patients with Turner Syndrome in Turkey: A Survey of 18 Pediatric Endocrinology Centers. *J Clin Res Pediatr Endocrinol* **2018,** *10* (3), 230-238.

26. Hou, W. H.; Chang, K. C.; Li, C. Y.; Ou, H. T., Dipeptidyl Peptidase-4 Inhibitor Use Is Associated with Decreased Risk of Fracture in Patients with Type 2 Diabetes: A Population-Based Cohort Study. *Br J Clin*

Pharmacol **2018,** *84* (9), 2029-2039.

27. Martinborough, E.; Shen, Y.; Oeveren, A.; Long, Y. O.; Lau, T. L.; Marschke, K. B.; Chang, W. Y.; Lopez, F. J.; Vajda, E. G.; Rix, P. J.; Viveros, O. H.; Negro-Vilar, A.; Zhi, L., Substituted 6-(1-Pyrrolidine)Quinolin-2(1h)-Ones as Novel Selective Androgen Receptor Modulators. *J Med Chem* **2007,** *50* (21), 5049-5052.

28. Medina-Franco, J. L.; Petit, J.; Maggiora, G. M., Hierarchical Strategy for Identifying Active Chemotype Classes in Compound Databases. *Chem Biol Drug Des* **2006,** *67* (6), 395-408.

29. Langdon, S. R.; Brown, N.; Blagg, J., Scaffold Diversity of Exemplified Medicinal Chemistry Space. *J Chem Inf Model* **2011,** *51* (9), 2174-2185.

30. Hu, Y.; Stumpfe, D.; Bajorath, J., Computational Exploration of Molecular Scaffolds in Medicinal Chemistry. *J Med Chem* **2016,** *59* (9), 4062-4076.

31. Delaisse, J. M.; Andersen, T. L.; Engsig, M. T.; Henriksen, K.; Troen, T.; Blavier, L., Matrix Metalloproteinases (Mmp) and Cathepsin K Contribute Differently to Osteoclastic Activities. *Microsc Res Tech* **2003,** *61* (6), 504-513.

32. Asagiri, M.; Sato, K.; Usami, T.; Ochi, S.; Nishina, H.; Yoshida, H.; Morita, I.; Wagner, E. F.; Mak, T. W.; Serfling, E.; Takayanagi, H., Autoamplification of Nfatc1 Expression Determines Its Essential Role in Bone Homeostasis. *J Exp Med* **2005,** *202* (9), 1261-1269.

33. Cheng, C. P.; Huang, H. S.; Hsu, Y. C.; Sheu, M. J.; Chang, D. M., A Benzamide-Linked Small Molecule Ndmc101 Inhibits Nfatc1 and Nf-Kappab Activity: A Potential Osteoclastogenesis Inhibitor for Experimental Arthritis. *J Clin Immunol* **2012,** *32* (4), 762-777.

34. Reginster, J. Y.; Sarkar, S.; Zegels, B.; Henrotin, Y.; Bruyere, O.; Agnusdei, D.; Collette, J., Reduction in Pinp, a Marker of Bone Metabolism, with Raloxifene Treatment and Its Relationship with Vertebral Fracture Risk. *Bone* **2004,** *34* (2), 344-351.

35. Ducy, P.; Karsenty, G., Two Distinct Osteoblast-Specific Cis-Acting Elements Control Expression of a Mouse Osteocalcin Gene. *Mol Cell Biol* **1995,** *15* (4), 1858-1869.

36. Xu, J.; Tan, J. W.; Huang, L.; Gao, X. H.; Laird, R.; Liu, D.; Wysocki, S.; Zheng, M. H., Cloning, Sequencing, and Functional Characterization of the Rat Homologue of Receptor Activator of Nf-Kappab Ligand. *J Bone Miner Res* **2000,** *15* (11), 2178-2186.

Table of Contents graphic

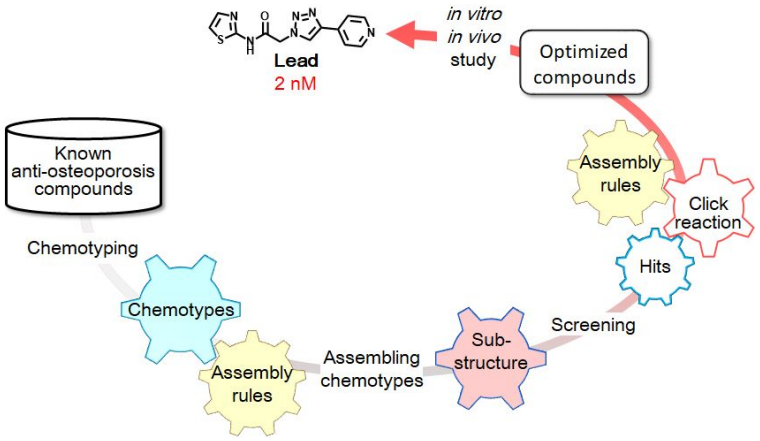

Figure 1

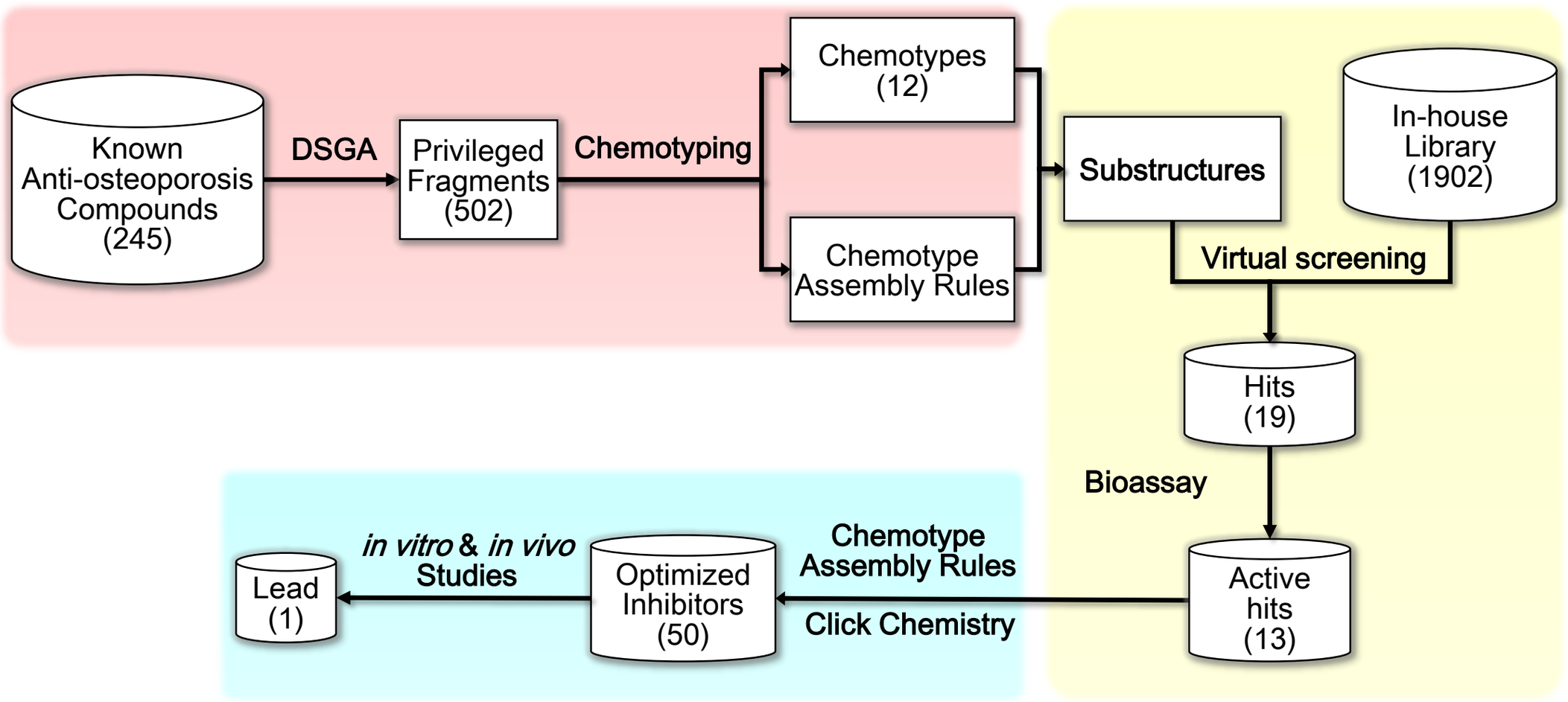
Known Anti-osteoporosis Compounds (245)
DSGA
Privileged Fragments (502)
Chemotyping
Chemotypes (12)
Chemotype Assembly Rules
Substructures
In-house Library (1902)
Virtual screening
Hits (19)
Bioassay
Active hits (13)
Chemotype Assembly Rules
Click Chemistry
Optimized Inhibitors (50)
in vitro & in vivo Studies
Lead (1)

Figure 2

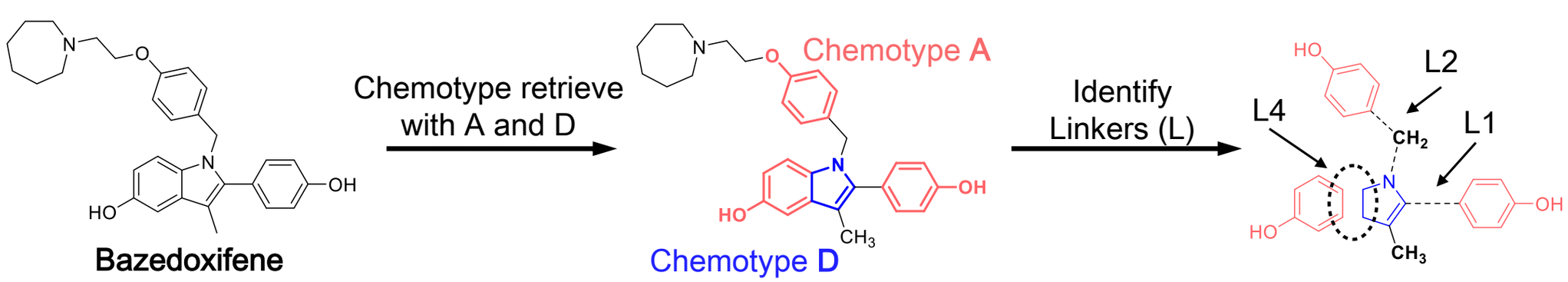

Linker 1 (L1)	Linker2 (L2)	Linker 3 (L3)	Linker 4 (L4)	Linker 5 (L5)
Coupling	A=C, N, O, S n = 0 ~ 3	X = O, N, S Y = O, N, S, C m, n = 0 - 1	Ring Fusing	Ring Merging

Figure 3

A

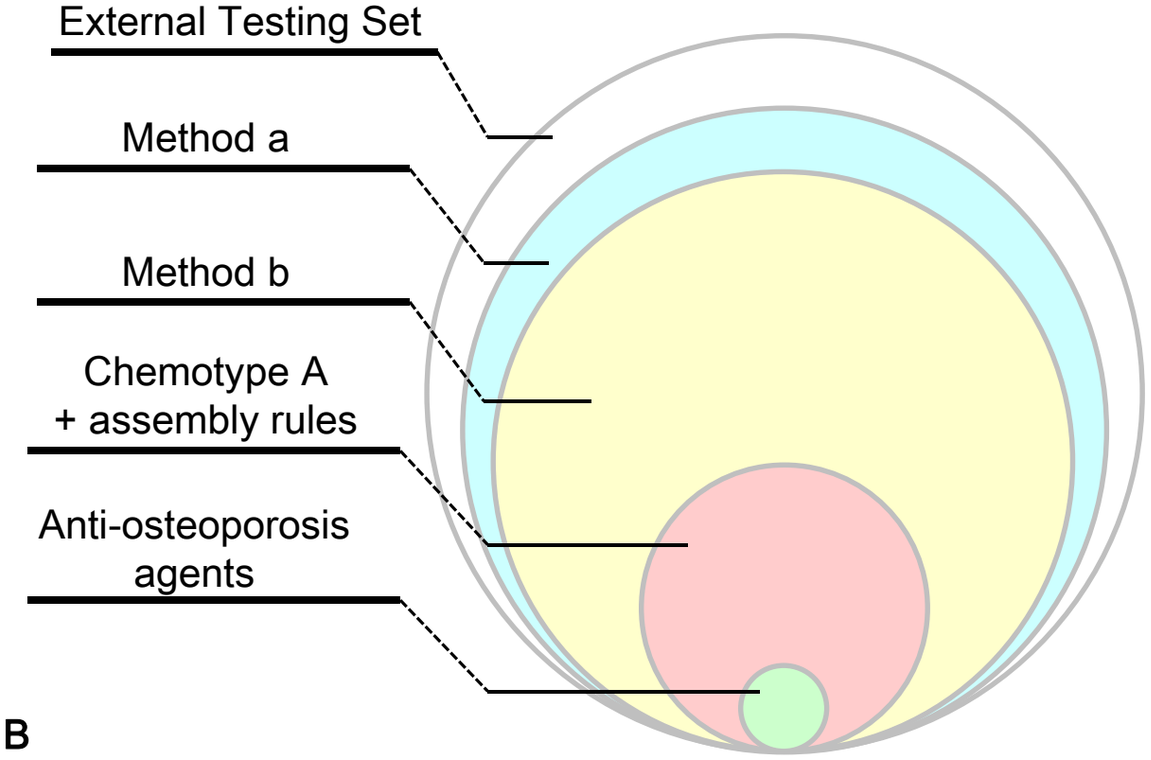

Parameters	Screening method		
	Method a	Method b	Chemotype A + assembly rules
D	8590	8590	8590
A	32	32	32
Ha	32	32	32
Ht	3630	3618	610
Hit rate	0.88%	0.88%	5.25%
EF	2.37	2.37	14.08

B

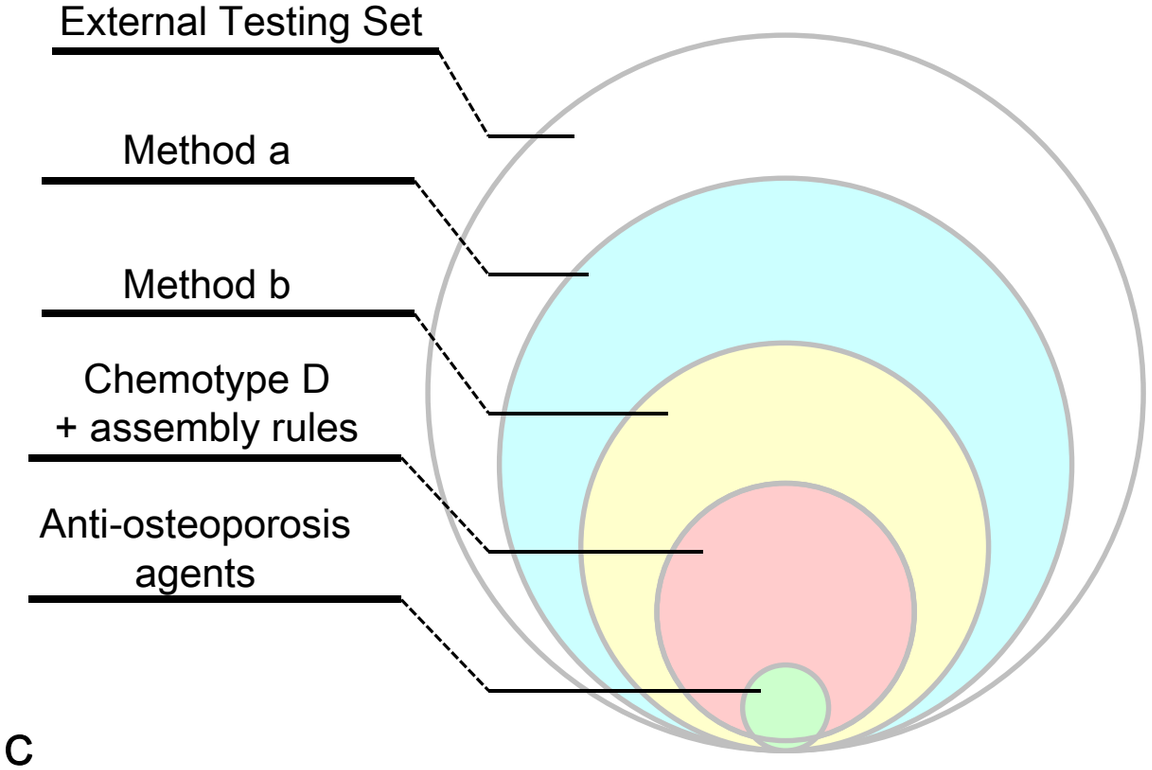

Parameters	Screening method		
	Method a	Method b	Chemotype D + assembly rules
D	8586	8586	8586
A	28	28	28
Ha	28	28	27
Ht	1960	1788	538
Hit rate	1.43%	1.57%	5.02%
EF	4.38	4.80	15.39

C

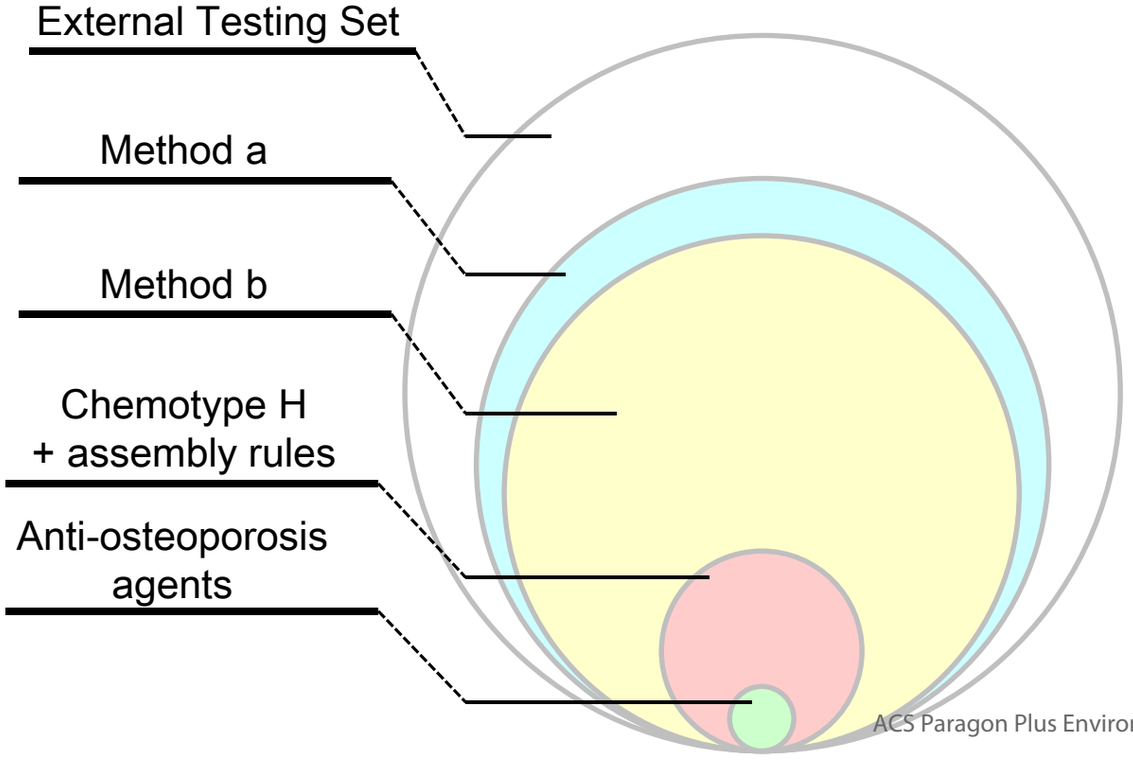

Parameters	Screening method		
	Method a	Method b	Chemotype H + assembly rules
D	8566	8566	8566
A	8	8	8
Ha	8	8	8
Ht	1774	1663	166
Hit rate	0.45%	0.48%	4.82%
EF	4.83	5.15	51.60

Figure 4

A

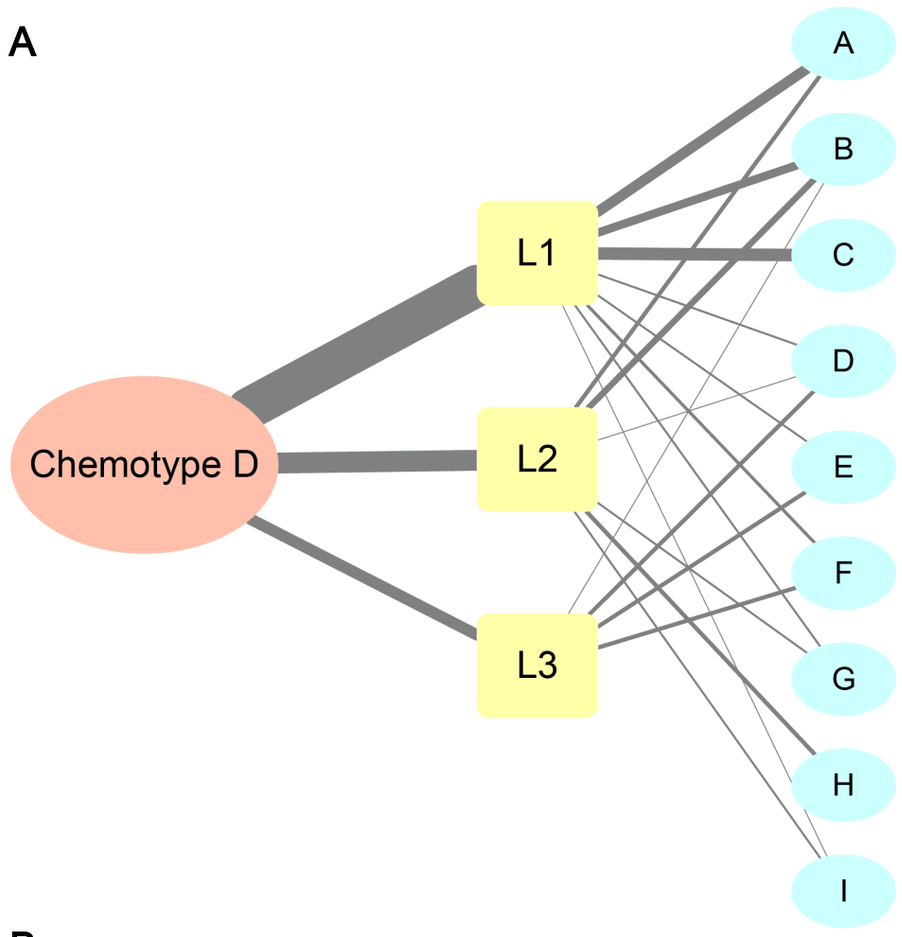

B

	A	B	C	D	E	F	G	H	I	J	K	L
L1	10	8	12	2	2	3	2	×	2	×	×	×
L2	4	6	×	1	×	×	2	4	2	×	×	×
L3	×	1	×	4	4	4	×	×	×	×	×	×

Figure 5

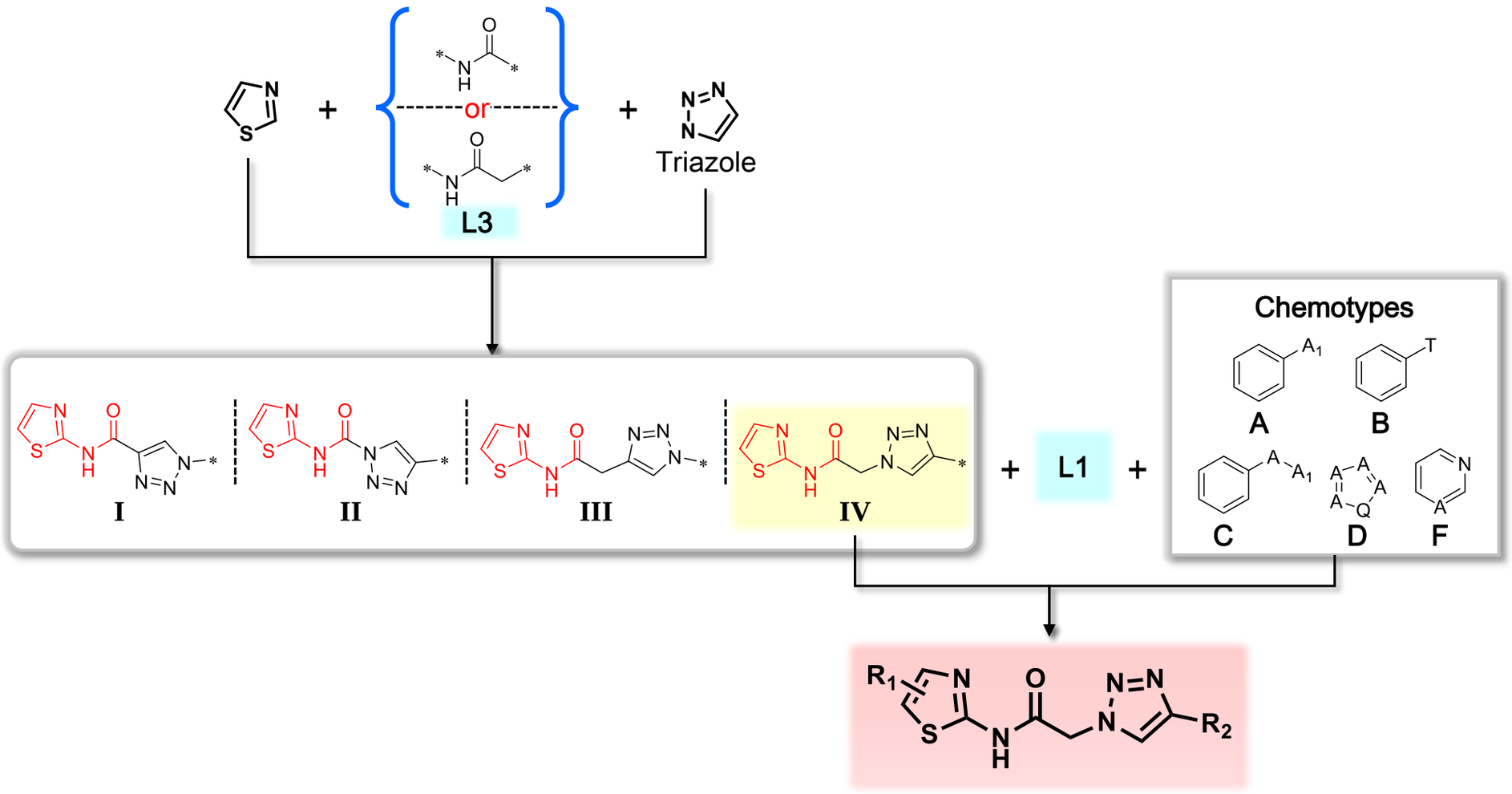

Figure 6

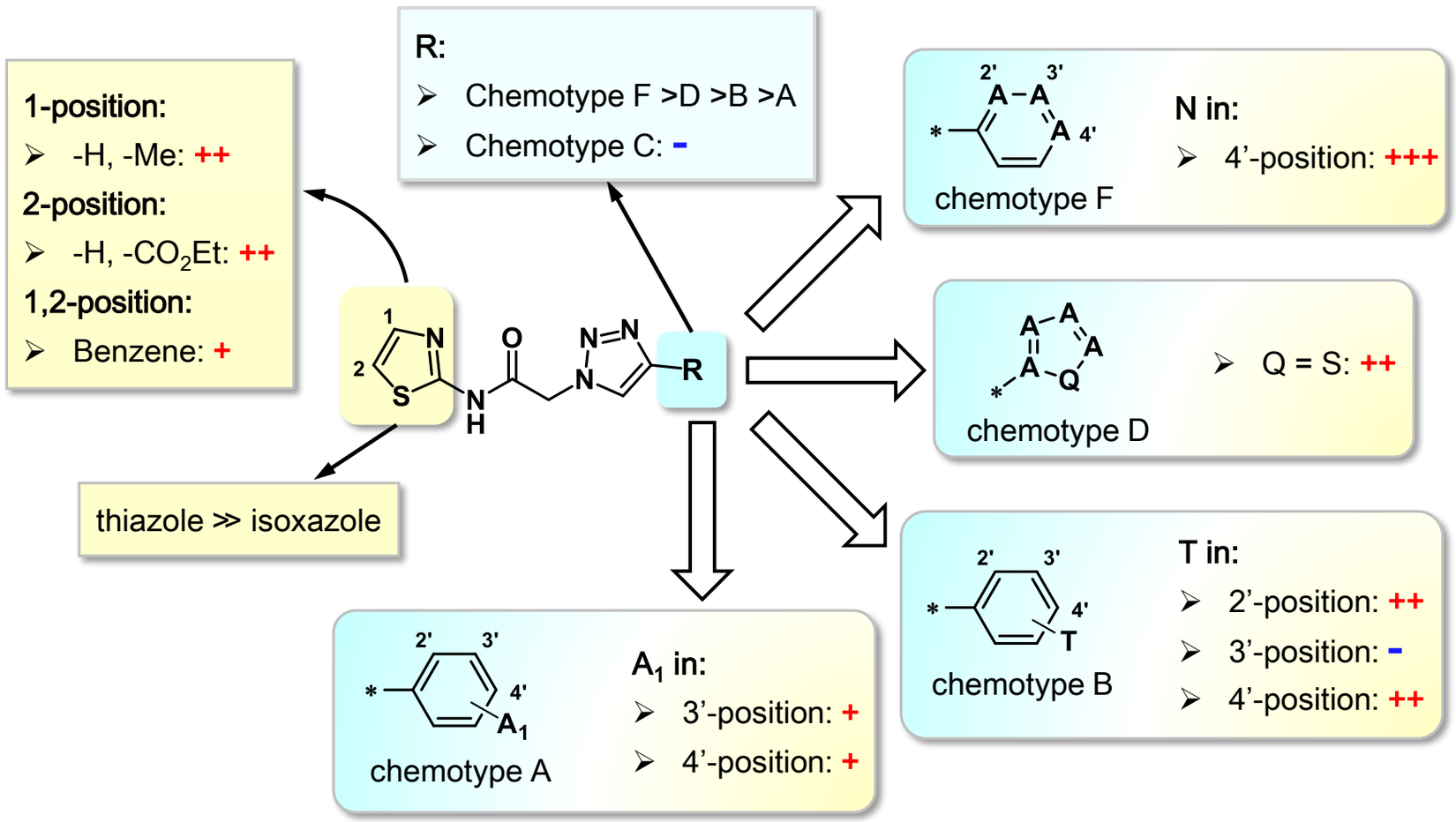

- non-activity + IC_{50} = 1 ~ 30 μM ++ IC_{50} = 0.1 ~ 1 μM +++ IC_{50} = 0.1 ~ 0.01 μM

Figure 7

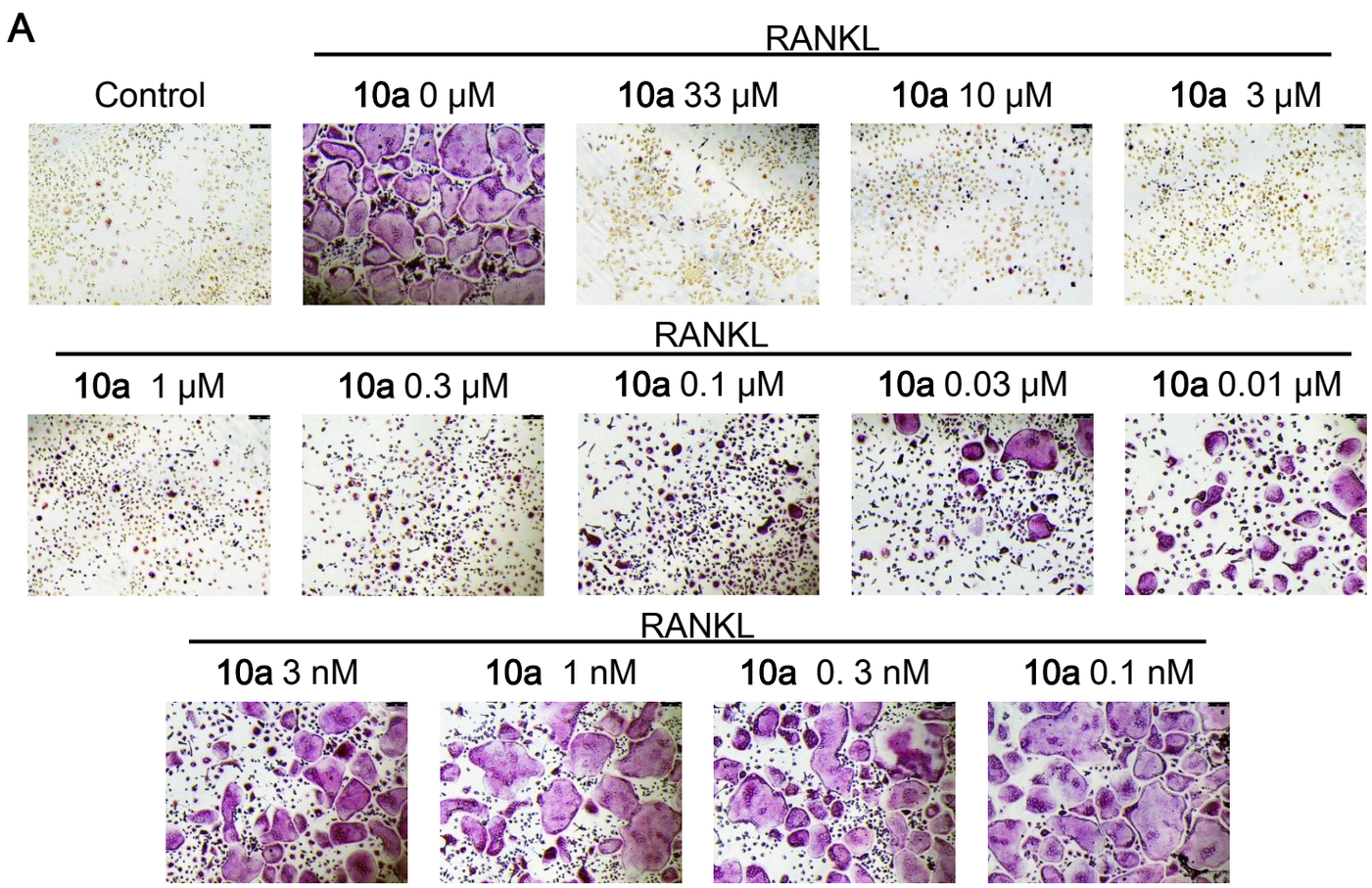
A
RANKL
Control
10a 0 μM
10a 33 μM
10a 10 μM
10a 3 μM
RANKL
10a 1 μM
10a 0.3 μM
10a 0.1 μM
10a 0.03 μM
10a 0.01 μM
RANKL
10a 3 nM
10a 1 nM
10a 0. 3 nM
10a 0.1 nM
B
TRAcP
NFATc1
MMP9
c-Fos
Control
+RANKL
RANKL+10a
C
Control
RANKL
RANKL
10a 1 μM
10a 0.1 μM
10a 0.01 μM
D
Control
10a
1 μM
10a
0.1 μM

Figure 8

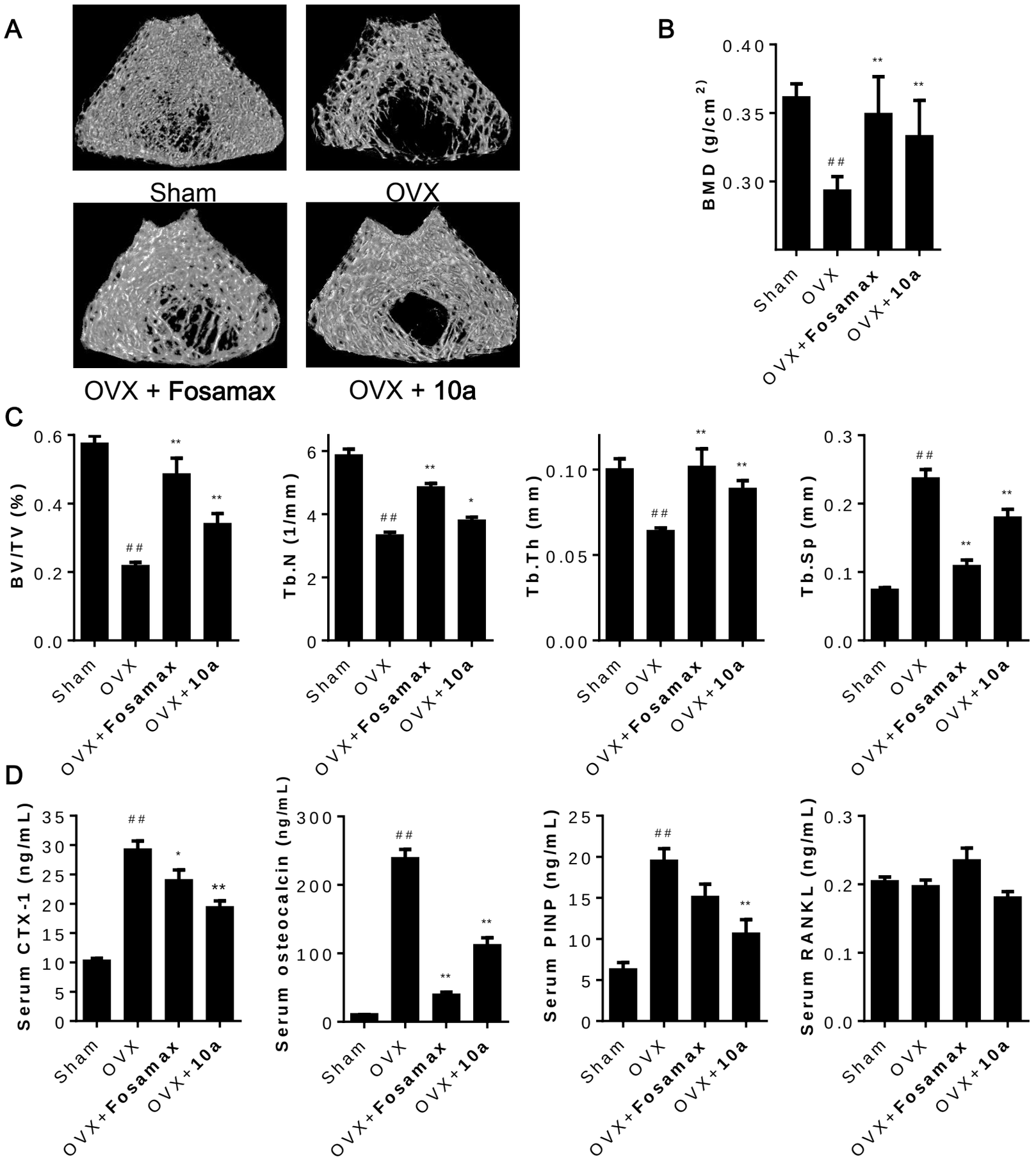
A
Sham
OVX
OVX + Fosamax
OVX + 10a
B
BMD (g/cm2)
0.40
0.35
0.30
Sham
OVX
OVX+Fosamax
OVX+10a
C
BV/TV (%)
Tb.N (1/mm)
Tb.Th (mm)
Tb.Sp (mm)
D
Serum CTX-1 (ng/mL)
Serum osteocalcin (ng/mL)
Serum PINP (ng/mL)
Serum RANKL (ng/mL)

TOC

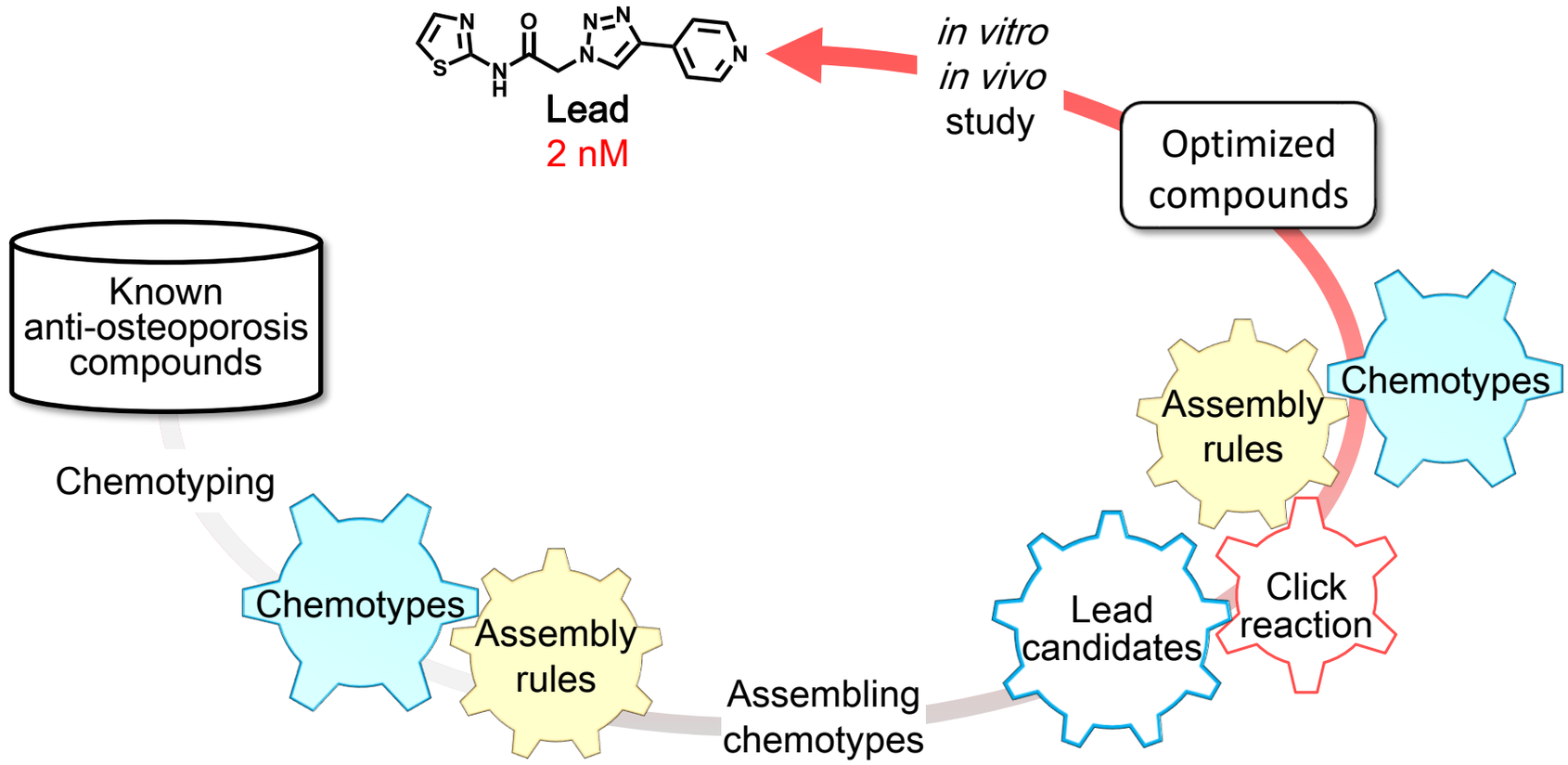
Lead
2 nM
in vitro
in vivo
study
Optimized
compounds
Known
anti-osteoporosis
compounds
Chemotyping
Chemotypes
Assembly
rules
Assembling
chemotypes
Lead
candidates
Click
reaction
Assembly
rules
Chemotypes